Molecular Pharmacology Fast Forward. Published on February 9, 2019 as DOI: 10.1124/mol.118.114744
This article has not been copyedited and formatted. The final version may differ from this version.

MOL # 114744

A comparison of the ability of Leu^8- and Pro^8-oxytocin to regulate intracellular Ca^{2+} and Ca^{2+}-activated K^+ channels at human and marmoset oxytocin receptors

Marsha L. Pierce, Suneet Mehrotra, Aaryn C. Mustoe, Jeffrey A. French, Thomas F. Murray

Department of Pharmacology, Creighton University School of Medicine, 2500 California Plaza, Omaha, NE 68178, USA (MLP, SM, TFM).

Department of Psychology, University of Nebraska Omaha, 6001 Dodge St., Omaha, NE 68182, USA (ACM, JAF).

Molecular Pharmacology Fast Forward. Published on February 9, 2019 as DOI: 10.1124/mol.118.114744
This article has not been copyedited and formatted. The final version may differ from this version.

Running Title: A comparison of Leu8- and Pro8-oxytocin signaling

Corresponding Author: Thomas F. Murray, Department of Pharmacology, Creighton University School of Medicine, 2500 California Plaza, Omaha, NE, 68178, U.S.A. Phone: 402-280-4076. Fax: 402-280-5762. E-mail: tfmurray@creighton.edu

Number of text pages: 27

Number of tables: 2

Number of figures: 4

Number of references: 75

Abstract word count: 249

Introduction word count: 703

Discussion word count: 1484

Supplementary tables: 5

Supplementary figures: 11

ABBREVIATIONS AA, amino acid; BAPTA-AM, 1,2-Bis(2-aminophenoxy)ethane-N,N,N′,N′-tetraacetic acid tetrakis(acetoxymethyl ester); BSA, bovine serum albumin; Ca^{2+}, calcium; CHO, Chinese hamster ovary; CI, confidence interval; CNS, central nervous system; EC_{50}, the half-maximal response; E_{MAX}, is the maximum response achievable; FMP, FLIPR membrane potential; GIRKs, G protein-coupled inwardly-rectifying potassium channels; GPCR, G protein-coupled receptor; hOTR, human oxytocin receptor; IC_{50}, is the half-inhibitory response; κOR-CHO, Kappa-opioid receptor expressing Chinese hamster ovary cells; Leu^8-OT, consensus mammalian oxytocin sequence; mOTR, marmoset oxytocin receptor; NWM, new world monkeys; OT, oxytocin; OTR, oxytocin receptor; K^+, potassium; Pro^8-OT, oxytocin sequence with proline in 8^{th} position; PKC, protein kinase C; PTX, pertussis toxin; Tg, thapsigargin

Molecular Pharmacology Fast Forward. Published on February 9, 2019 as DOI: 10.1124/mol.118.114744
This article has not been copyedited and formatted. The final version may differ from this version.

ABSTRACT

The neurohypophyseal hormone oxytocin (OT) regulates biological functions in both peripheral tissues and the central nervous system (CNS). In the CNS, OT influences social processes including peer relationships, maternal-infant bonding and affiliative social relationships. In mammals, the nonapeptide OT structure is highly conserved with leucine in the 8th position (Leu^8-OT). In marmosets (*Callithrix*) a nonsynonymous nucleotide substitution in the *OXT* gene codes for proline in the 8th residue position (Pro^8-OT). OT binds to its cognate G protein-coupled receptor (OTR) and exerts diverse effects, including stimulation (G_s) or inhibition ($G_{i/o}$) of adenylyl cyclase, stimulation of potassium channel currents (G_i) and activation of phospholipase C (G_q). CHO cells expressing marmoset (mOTR) or human (hOTR) oxytocin receptors were used to characterize OT signaling. At mOTR Pro^8-OT was more efficacious than Leu^8-OT in measures of G_q activation with both peptides displaying subnanomolar potencies. At hOTR, neither potency nor efficacy of Pro^8-OT and Leu^8-OT differed with respect to G_q signaling. In both mOTR- and hOTR-expressing cells Leu^8-OT was more potent and modestly more efficacious than Pro^8-OT in inducing hyperpolarization. In mOTR cells Leu^8-OT-induced hyperpolarization was modestly inhibited by pretreatment with pertussis toxin (PTX) consistent with a minor role for $G_{i/o}$-activation; however, the Pro^8-OT response in mOTR and hOTR cells was PTX-insensitive. These findings are consistent with membrane hyperpolarization being largely mediated by a G_q signaling mechanism leading to Ca^{2+}-dependent activation of K^+ channels. Evaluation of the influence of apamin, charybdotoxin, paxilline and TRAM-34 demonstrated involvement of both intermediate and large conductance Ca^{2+}-activated K^+ channels.

Molecular Pharmacology Fast Forward. Published on February 9, 2019 as DOI: 10.1124/mol.118.114744
This article has not been copyedited and formatted. The final version may differ from this version.

INTRODUCTION

Oxytocin (OT) is a nonapeptide that regulates a host of physiological functions both peripherally (e.g., uterine contraction, lactation) and centrally (e.g., social behavior). OT is synthesized in the magnocellular neurons of the supraoptic and paraventricular nuclei of the hypothalamus, and OT neurons primarily project to the posterior pituitary where OT is released into the bloodstream (Ludwig & Leng, 2006). OT neurons also project to multiple regions within the 'social brain' (Stoop, 2014). These latter OT projections are thought to be responsible for the modulation of many behaviors including social recognition/memory, sexual behavior, parental care, pair-bond formation and maintenance, and cooperation and aggression (Insel et al., 2010; Johnson & Young, 2015). Dysfunction in OT signaling has also been widely reported in mental health outcomes where social deficits are commonly observed such as schizophrenia, and depression/anxiety. Consequently, OT has received considerable interest as a therapeutic for these disorders with mixed success (Guastella & Hickie, 2016; Parker et al., 2017; Young & Barrett, 2015).

OT-like nonapeptides are highly conserved signaling molecules that activate G-protein coupled receptors (GPCRs). OT binds primarily to the oxytocin receptor (OTR), and to a lesser extent the related nonapeptide vasopressin receptors (Gimpl & Fahrenholz, 2001; Manning et al., 2008). OTR promiscuously couples to and activates multiple G-proteins producing diverse effects on cellular function including inhibition of adenylyl cyclase ($G_{i/o}$), stimulation of potassium channel currents (G_i) and activation of phospholipase C (G_q) (Reversi, Cassoni, & Chini, 2005). OTR activation also leads to a variety of signaling responses that suggest OT activation may preferentially bias specific

Molecular Pharmacology Fast Forward. Published on February 9, 2019 as DOI: 10.1124/mol.118.114744
This article has not been copyedited and formatted. The final version may differ from this version.

G-protein pathways that vary across cell types both within the brain and in the periphery. For example, activation of neural OTRs that generate pulsatile OT secretion is mediated by G_q activation (Wang & Hatton, 2007), while in myometrial cells the mobilization of Ca^{2+} and GTP hydrolysis are mediated by both $G_{i/o}$ and G_q activation (Phaneuf et al., 1993).

Despite the high degree of conservation of the OT ligand among most mammals, many New World monkeys (NWMs) possess OT sequence modifications that have evolved from the ancestral mammalian OT sequence (Cys-Tyr-Ile-Gln-Asn-Cys-Pro-**Leu**-Gly; Leu^8-OT). Thus far, five additional OT-like variants have been identified with variability in amino acids (AA) mainly at position 8, but also at positions 2 and 3 (Lee et al., 2011; Ren et al., 2015; Vargas-Pinilla et al., 2015; Wallis, 2012). The most common OT variant is a Leu-to-Pro substitution at the 8^{th} AA position (Pro^8-OT). This substitution significantly alters the linear portion of the ligand's three-dimensional architecture, whereby the formation of Pro-Pro polyproline helix in the linear portion of the OT ligand could potentially lead to changes in OT interaction with the OTR with attendant alteration in potency and/or efficacy (Geisler & Chmielewski, 2009; Zingg & Laporte, 2003).

Differences between OT and the related nonapeptide vasopressin (which differs in AA positions 3 and 8) show select ligand recognition with specific portions of the OTR and V1aR, potentially suggesting important OTR recognition features that could change as a function of a Leu-to-Pro substitution in position 8 (Chini et al., 1995; Chini et al., 1996; Zingg & Laporte, 2003). OT ligand variants are also of interest because these ligands show significant co-evolution with corresponding OTR sequence structures, and a significant association with the presence of social phenotypes including social monogamy and paternal care in primates (Ren et al., 2015; Vargas-Pinilla et al., 2015),

Molecular Pharmacology Fast Forward. Published on February 9, 2019 as DOI: 10.1124/mol.118.114744
This article has not been copyedited and formatted. The final version may differ from this version.

and these social phenotypes are known to be influenced by exogenous OT treatments (French et al., 2016). The association between OT/OTR structures with social behavior in NWMs raises the possibility that OT-related phenotypic differences might be a consequence of functional selectivity with respect to the signaling properties associated with OT analog (e.g., Pro^8-OT) activation of OTRs. Currently, there is limited information regarding signaling profiles of OT analogs at human and marmoset oxytocin receptors.

To assess whether OT/OTR variability results in altered pharmacological properties of OT ligands, we stably transfected CHO cells expressing human (hOTR) or marmoset OTRs (mOTR) and examined the resulting activation of OT-OTR signaling pathways. We evaluated whether OT ligand variation resulted in distinct activation of different G-protein mediated cell-signaling pathways ($G_{i/o}$ and G_q) in hOTR and mOTR expressing cells as assessed by elevation of intracellular Ca^{2+} or alteration in membrane potential.

Molecular Pharmacology Fast Forward. Published on February 9, 2019 as DOI: 10.1124/mol.118.114744
This article has not been copyedited and formatted. The final version may differ from this version.

MATERIALS AND METHODS

Chinese hamster ovary (CHO) cell cultures. Wild-type Chinese hamster ovarian-K1 (CHO-K1) cells were purchased from ATCC (CCL-61) and cultured in Ham's F12 (Hyclone SH30026.01), 10% fetal bovine serum (FBS) (Atlanta Biologicals S11550), 1.5% HEPES 1M Solution (Hyclone SH30231.01), 1% Penicillin-Streptomycin (10,000 U/mL; Life Technologies 15140-163). Human oxytocin receptor (hOTR) expressing CHO-K1 cell lines were purchased from Genscript (M00195). Marmoset oxytocin receptor (mOTR) plasmid was purchased from Genscript and stably-transfected into CHO-K1 cells. hOTR and mOTR expressing cells were cultured in Ham's F12 (Hyclone SH30026.01), 10% FBS (Atlanta Biologicals S11550), 1.5% HEPES 1M Solution (Hyclone SH30231.01), 1% Penicillin-Streptomycin (10,000 U/mL; Life Technologies 15140-163) and 400 mg/mL G418 (RPI Corp. G64000-5.0). Kappa-opioid receptor (κOR) expressing CHO cells (κOR-CHO) were cultured in RMPI-1640 medium supplemented with 10% FBS (Atlanta Biologicals S11550). Cells were cultured at 37°C in 5% CO_2 and 90% humidity.

CHO cell stable transfection and selection of clones. CHO-K1 cells (1 x 10^6) were electroporated with 1.5 µg of vector encoding marmoset oxytocin receptor (mOTR) plasmid (Genscript). After transfection, cells were seeded on 10 cm plates, and grown under antibiotic pressure 400 mg/mL G418 (RPI Corp. G64000-5.0) for 72 hours. The clones were picked using cloning cylinders (Corning 3166-10), 50 µl of 0.05% trypsin (GIBCO 25300-054) added to the cells/colony and detached by pipetting 2-3 times. Dissociated cells diluted in 100 ml media and plated in 24 well plates (~ 1 cell/well). The cells were allowed to grow under antibiotic pressure for 3 weeks, with media change

Molecular Pharmacology Fast Forward. Published on February 9, 2019 as DOI: 10.1124/mol.118.114744
This article has not been copyedited and formatted. The final version may differ from this version.

every 72 hours. Five clones were picked for FMP assay. Among all five clones, Clone 2 showed maximum responses to Leu^8-OT and Pro^8-OT in decreasing the FMP blue fluorescence and was selected for further studies.

Drugs. Leu^8-OT (American Peptide Company 66-0-52) and Pro^8-OT (Anaspec 58863) was reconstituted in DMSO (Sigma-Aldrich D4540). Charybdotoxin (Sigma-Aldrich C7802) was reconstituted in ultrapure water. BAPTA-AM (Sigma-Aldrich A1076), M119K (Developmental Therapeutics Program, National Cancer Institute 1198893), NS-1619 (Sigma-Aldrich N170), Paxilline (Sigma-Aldrich P2928), SKA-31 (Sigma-Aldrich S5573), thapsigargin (Sigma-Aldrich T9033), and TRAM-34 (Sigma-Aldrich T6700) were reconstituted in DMSO. Pertussis toxin (Sigma-Aldrich P7208) was reconstituted in ultrapure water with 5 mg/mL bovine serum albumin (Fisher Scientific BP1600-100). Dynorphin A (1-13) amide (American Peptide 26-4-51A) was dissolved in 25 mM Tris at pH 7.4. Apamin (Sigma-Aldrich A1289) was reconstituted in 0.05 M acetic acid.

Intracellular Calcium Mobilization Assay. The effect of oxytocin addition on intracellular calcium mobilization was examined using Fluo3-AM fluorescence (Molecular Probes F1241) monitored with a FLIPR2 plate reader (Molecular Devices, Sunnyvale, CA). FLIPR operates by illuminating the bottom of a 96-well microplate with an air-cooled laser and measuring the fluorescence emissions from cell-permeant dyes in all 96 wells simultaneously using a cooled CCD camera. This instrument is equipped with an automated 96-well pipettor, which can be programmed to deliver precise quantities of solutions simultaneously to all 96 culture wells from two separate 96-well source plates.

Molecular Pharmacology Fast Forward. Published on February 9, 2019 as DOI: 10.1124/mol.118.114744
This article has not been copyedited and formatted. The final version may differ from this version.

Cells were plated at 0.3 million cells/mL in 96-well plates (MidSci P9803) and cultured overnight in culture media at 37°C in 5% CO_2 and 95% humidity. On the day of assay, growth medium was aspirated and replaced with 100 µl dye-loading medium per well containing 4 µM Fluo-3 AM and 0.04% pluronic acid (Molecular Probes P3000MP) in Locke's buffer (8.6 mM HEPES, 5.6 mM KCl, 154 mM NaCl, 5.6 mM glucose, 1.0 mM $MgCl_2$, 2.3 mM $CaCl_2$ pH 7.4). Cells were incubated for 1 h at 37°C in 5% CO2 and 95% humidity and then washed four times in 180µl fresh Locke's buffer using an automated microplate washer (Bio-Tek Instruments Inc., VT). Baseline fluorescence was recorded for 60 s, prior to a 20 µl addition of various concentrations of Leu^8-OT and Pro^8-OT. Cells were excited at 488 nm and Ca^{2+}-bound Fluo-3 emission was recorded at 538 nm at 2 s intervals for an additional 200 s.

To assess the role of intracellular calcium in the OT mobilization of calcium, the sarco/endoplasmic reticulum Ca^{2+} ATPase (SERCA) inhibitor thapsigargin was used to rapidly deplete intracellular calcium stores. Thapsigargin inhibition of calcium mobilization in prostrate cancer cells is complete in less than five minutes (Sehgal et al., 2017). Cells were incubated in 100 µl dye-loading medium per well containing 4µM Fluo-3 AM and 0.04% pluronic acid in Locke's buffer (8.6 mM HEPES, 5.6 mM KCl, 154 mM NaCl, 5.6 mM glucose, 1.0 mM $MgCl_2$, 2.3 mM $CaCl_2$, 0.5 mM probenecid; pH 7.4). Cells were incubated at 37°C in a 5% CO2 and 95% humidity for 60 min prior washing four times in 180 µl Locke's buffer and 10 µl addition of thapsigargin (1 µM final concentration) and incubated for an additional five minutes. Intracellular calcium mobilization assays were performed as described above.

Molecular Pharmacology Fast Forward. Published on February 9, 2019 as DOI: 10.1124/mol.118.114744
This article has not been copyedited and formatted. The final version may differ from this version.

Membrane Potential Assay. To assess changes in membrane potential the FLIPR Membrane Potential Assay (FMP blue; Molecular Probes F1241) was used. Confluent cells plated at 0.3 million cells/ml in 96-well plates (MidSci P9803) and cultured overnight in culture media at 37°C in 5% CO_2 and 95% humidity. Growth medium was removed and replaced with 190 µl per well of FMP Blue in Locke's buffer (8.6 mM HEPES, 5.6 mM KCl, 154 mM NaCl, 5.6 mM glucose, 1.0 mM $MgCl_2$, 2.3 mM $CaCl_2$ pH 7.4). Cells were incubated at 37°C in 5% CO_2 and 95% humidity for 45 min. Baseline fluorescence was recorded for 60 s, prior to a 10 µl addition of log concentrations of Leu^8-OT and Pro^8-OT. Cells were excited at 530 nm and emission was recorded at 565 nm at 2 s intervals for an additional 200 s.

To ensure the veracity of comparisons of EC_{50} and E_{MAX} values of OT variants, all compounds were evaluated in parallel on the same 96-well plate, with the same split of cells and with identical reagent solutions. This experimental design was used for all OT peptide comparisons throughout this study using both human and marmoset OTR expressing cells. Inasmuch as all assays were performed in the same CHO cell line, we can exclude differences in cellular context as a source of observed differences in peptide potency or efficacy.

To assess the role $G_{i/o}$ in the OT ligand-induced membrane hyperpolarization cells were incubated overnight with pertussis toxin (PTX) to inactivate $G_{i/o}$ (Zhou et al., 2007). Cells were plated at 125,000 cells/mL in 96-well plates. PTX (150 ng/ml) was added 24 hours after plating and incubated for an additional 24 hours. Membrane potential assay was performed as described above. To confirm the influence of PTX on a known $G_{i/o}$ mediated response, the effect of PTX on kappa-opioid receptor mediated

hyperpolarization was used as a positive control (Murthy & Makhlouf, 1996). κOR-CHO were used for these experiments. The PTX assays were performed as described above for mOTR- and hOTR-expressing CHO cells, except for stimulation with dynorphin rather than OT analogs.

M119K is a Gβγ inhibitor (Kirui et al., 2010). If Leu^8-OT ligand-induced membrane hyperpolarization cells is partially mediated by downstream Gβγ activation of GIRK channels, then it should be partially sensitive to M119K. Cells were incubated at 37°C in a 5% CO2 and 95% humidity for 35 min prior to a 10 µl addition of M119K. Cells were incubated for an additional 10 min after drug addition. Membrane potential assays were performed as described above.

To assess potential OT ligand-induced membrane hyperpolarization through Ca^{2+}-activated potassium channels, we tested four inhibitors targeting distinct Ca^{2+}-activated potassium channel subtypes. G_q-mediated activation of protein kinase-C (PKC) causes an increase in cytosolic calcium (Ritter & Hall, 2009) with attendant activation of Ca^{2+} sensitive potassium channels. Ca^{2+}-activated potassium channels are separated into three subtypes of large (BK_{Ca}), intermediate (IK_{Ca}), and small conductance (SK_{Ca}) channels (Vergara et al.,1998). Paxilline is a selective inhibitor of the BK_{Ca} channel (Sanchez & McManus, 1996), while charybdotoxin is an inhibitor various IK_{Ca} (Anderson, Harvey, Rowan, & Strong, 1988; Ishii et al., 1997) and BK_{Ca} channels (Qiu et al., 2009). TRAM-34 is a selective inhibitor of the IK_{Ca} channel, $K_{Ca}3.1$ that has been shown to reach maximum blockade in 3-6 minutes (Nguyen et al., 2017; Staal et al., 2017). In COS-7 cells, 100 nM TRAM-34 blocked ~90% of IK_{Ca} currents (Wulff et al., 2000). Apamin is a selective inhibitor of SK_{Ca} channels (Blatz & Magleby,

Molecular Pharmacology Fast Forward. Published on February 9, 2019 as DOI: 10.1124/mol.118.114744
This article has not been copyedited and formatted. The final version may differ from this version.

1986; Lamy et al., 2010). In HEK cells expressing SK_{Ca} channels $K_{Ca}2.2$ and $K_{Ca}2.3$ addition of 100 nM concentrations of apamin blocked ~70% and 80% of of $K_{Ca}2.2$ and $K_{Ca}2.3$-mediated currents (Lamy et al., 2010). Cells were incubated at 37°C in a 5% CO2 and 95% humidity for 35 min prior to a 10 µl addition of charybdotoxin, paxilline TRAM-34, and/or apamin. Cells were incubated for an additional 10 min after drug addition. Membrane potential assays were performed as described above.

NS-1619 is a BK_{Ca} channel activator (Edwards, et al. 1994; Lee, Rowe, & Ashford, 1995). NS-1619 (30 µM) opens BK_{Ca} channels in horizontal cells of rats and mice (Sun et al., 2017). If changes in intracellular calcium are responsible for activation of the BK_{Ca}, the response should be NS-1619 sensitive. Cells were incubated at 37°C in a 5% CO2 and 95% humidity for 35 min prior to a 10 µl addition of paxilline. Cells were incubated for an additional 10 min after paxilline addition. Membrane potential assays were performed as described above, with the exception of challenge with NS-1619 rather than OT analogs.

SKA-31 is an activator of IK_{Ca} channel $K_{Ca}3.1$ (Christophersen & Wulff, 2015; Sankaranarayanan et al., 2009). If changes in intracellular calcium are responsible for the activation of $K_{Ca}3.1$, the response should be SKA-31 sensitive. Cells were incubated at 37°C in a 5% CO2 and 95% humidity for 35 min prior to a 10 µl addition of TRAM-34. Cells were incubated for an additional 10 min after TRAM-34 addition. Membrane potential assays were performed as described above, with the exception of stimulation with SKA-31 rather than OT analogs.

1,2-Bis(2-aminophenoxy)ethane-N,N,N′,N′-tetraacetic acid tetrakis(acetoxymethyl ester) (BAPTA-AM) is an intracellular calcium chelator (Strayer, Hoek, Thomas, &

Molecular Pharmacology Fast Forward. Published on February 9, 2019 as DOI: 10.1124/mol.118.114744
This article has not been copyedited and formatted. The final version may differ from this version.

White, 1999). If changes in intracellular calcium are responsible for activation of the Ca^{2+}-activated potassium channels, the response should be BAPTA-AM sensitive. Cells were incubated at 37°C in a 5% CO2 and 95% humidity for 35 min prior to a 10 µl addition of BAPTA-AM. Cells were incubated for an additional 10 min after drug addition.

To assess the role of intracellular calcium in OT ligand-induced changes in membrane potential, thapsigargin was used. Cells were incubated at 37°C in a 5% CO2 and 95% humidity for 40 min prior to a 10 µl addition of thapsigargin. Cells were incubated for an additional 5 min after drug addition.

Data Analysis. All concentration-response data were analyzed and graphs generated using GraphPad Prism (San Diego, CA, U.S.A.) software. EC_{50} and E_{MAX} values for OT peptide-stimulated increases in fluo-3 fluorescence or decreases in FMP Blue fluorescence were determined by nonlinear regression least-squares fitting of a logistic equation to the peptide concentration versus fluorescence area under the curve data. The 95% confidence intervals for all EC_{50}/IC_{50} and E_{MAX} were used to assess differences in potency/efficacy. R^2 was used to assess goodness of fit. A one-way ANOVA was performed with Sidek's multiple comparisons to determine statistical significance and the adjusted p-values reported.

Molecular Pharmacology Fast Forward. Published on February 9, 2019 as DOI: 10.1124/mol.118.114744
This article has not been copyedited and formatted. The final version may differ from this version.

RESULTS

OT Analogs Induce G_q-mediated Intracellular Calcium Mobilization

G_q-mediates intracellular calcium mobilization by activation of PLCβ with attendant inositol phosphate and diacylglycerol production (Ritter & Hall, 2009). To assess OTR activation of G_q, functional assays were performed using fluo-3 AM as a calcium indicator dye. We asked whether Leu^8-OT, found in most mammals, and Pro^8-OT, found in many NWMs, show differential mobilization of intracellular Ca^{2+} upon activation of mOTRs. In mOTR CHO cells, we found that the two OT ligands produced a concentration-dependent elevation of intracellular calcium with similar potencies (EC_{50}), but the cognate ligand Pro^8-OT was more efficacious (E_{MAX}) than Leu^8-OT (Figure 1A-C; Table 1). In contrast, in hOTR CHO cells we found that the two OT ligands showed similar potencies and efficacies in increasing intracellular calcium concentration (Figure 1D-F, Table 1). The absence of a Leu^8-OT effect on calcium concentration in non-transfected CHO-K1 cells demonstrated that the OT peptide effects observed in transfected cell lines required mOTR and hOTR expression (Supplementary Figure 1).

Thapsigargin is a potent inhibitor of the sarco/endoplasmic reticulum calcium ATPase (SERCA), that is responsible for maintaining the gradient between the low calcium cytosol and the sarco/endoplasmic reticulum high calcium storage. Inhibition of the SERCA pump results in a depletion of intracellular calcium stores (Dravid & Murray, 2004; Quynh Doan & Christensen, 2015). To confirm the role of intracellular calcium stores in OT-mediated calcium influx, cells were pretreated cells with thapsigargin. In control mOTR and hOTR CHO cells Leu^8-OT and Pro^8-OT again produced concentration-dependent increases in intracellular calcium; however, pretreatment with

Molecular Pharmacology Fast Forward. Published on February 9, 2019 as DOI: 10.1124/mol.118.114744
This article has not been copyedited and formatted. The final version may differ from this version.

thapsigargin abrogated this response in CHO cells expressing both mOTR and hOTR for both OT analogs (Supplementary Figure 2). Together these data demonstrated that intracellular calcium stores represent the source of OT-mediated elevation cytosolic calcium levels.

OT Analog-Induced Changes in Membrane Potential are Dependent on G_q Mediated Calcium Mobilization

OT analog activation of OTR and coupling to G_i have been shown to stimulate K^+ channel conductances with attendant cellular hyperpolarization (Gravati et al., 2010; Phaneuf et al., 1993; Ritter & Hall, 2009). To assess potential OTR activation of K^+ channel conductance we performed functional assays using the membrane potential-sensitive dye, FMP blue. The FMP blue dye is a lipophilic, anionic, bis-oxonol-based dye that distributes across the cell membrane as a function of membrane potential and displays depolarization-induced increased fluorescence emission after binding to intracellular proteins, or decreased fluorescence following hyperpolarization-induced egress from cells (Baxter et al., 2002; Whiteaker et al., 2001). In mOTR CHO cells both Leu^8-OT and Pro^8-OT produced concentration-dependent decreases in FMP Blue fluorescence consistent with a hyperpolarization response. Leu^8-OT showed substantially greater potency compared to Pro^8-OT in the observed changes in membrane potential with the two OT ligands showing comparable efficacies (Figure 2A-C; Table 2). A similar pattern was observed in hOTR CHO cells with Leu^8-OT displaying greater potency than Pro^8-OT with regard to changes in membrane potential (Figure 2D-F; Table 2). The absence of Leu^8-OT and Pro^8-OT effects on membrane

Molecular Pharmacology Fast Forward. Published on February 9, 2019 as DOI: 10.1124/mol.118.114744
This article has not been copyedited and formatted. The final version may differ from this version.

potential in non-transfected CHO-K1 cells again demonstrated the requirement for mOTR and hOTR transfection in the observed hyperpolarization responses to OT ligands (Supplementary Figure 3).

Several classes of G-protein alpha subunits including, G_i and G_o, can be mono-ADP-ribosylated by the exotoxin from the gram-negative bacterium *Bordetella pertussis*. Pertussis toxin (PTX) catalyzes the covalent transfer of an ADP-ribose from NAD+ to a cysteine residue four amino acids from the carboxytermini of these alpha subunits (Murray, 1993). This ADP-ribosylation disrupts the coupling between G-protein coupled receptors (GPCR) and PTX-sensitive G-proteins and therefore potentially interfering with responses to agonists such as OT. We tested mOTR CHO cells and observed that PTX treatment partially affected Leu^8-OT-mediated hyperpolarization with a significant 31.9% reduction in efficacy, In control cells, the Leu^8-OT E_{MAX} was 3590 (95% CI 3088 to 4093), whereas in PTX-pretreated cells the E_{MAX} was 2446 (95% CI 1893 to 2999; Supplementary Figure 4A,C; Figure 3A). In contrast, in hOTR CHO cells pretreatment with PTX did not significantly inhibit Leu^8-OT-mediated hyperpolarization (Figure 3C; Supplementary Figure 4E,G; Supplementary Table 1). PTX treatment did not affect Pro^8-OT-induced hyperpolarization in either mOTR expressing (Figure 3B; Supplementary Figure 4B,D) or hOTR CHO cells (Figure 3D; Supplementary Figure 4F,H). These data demonstrate that in mOTR CHO cells Leu^8-OT-induced hyperpolarization is partially sensitive to PTX. The insensitivity of Pro^8-OT in mOTR and hOTR CHO cells to PTX indicates a lack of involvement of G_i mediated activation of G protein-coupled inwardly-rectifying potassium channels (GIRKs) in the observed changes in membrane potential. In contrast, the partial sensitivity of Leu^8-OT-induced

Molecular Pharmacology Fast Forward. Published on February 9, 2019 as DOI: 10.1124/mol.118.114744
This article has not been copyedited and formatted. The final version may differ from this version.

changes in membrane potential in mOTR-expressing cells suggests that both G_i-mediated and PTX-insensitive pathways are involved in the hyperpolarization in response to this peptide.

We used a kappa-opioid receptor expressing CHO cell line (κOR-CHO) as a positive control to demonstrate the ability of PTX to disrupt G-protein coupling to a GPCR. κORs couple to the PTX substrate G_i. Dynorphin A 1-13-NH_2 was used as the κOR agonist for these experiments. Dynorphin A 1-13-NH_2 produced a robust hyperpolarization response in control κOR-CHO cells, and this response was abrogated in PTX pretreated cells (Supplementary Figure 5). These data demonstrate the effectiveness of PTX in disrupting GPCR coupling to G_i.

PTX disrupts GPCR interaction with sensitive G proteins thereby interrupting downstream Gα and Gβγ-dependent signaling. To further assess the partial G_i mediation of Leu^8-OT-induced changes in membrane potential in mOTR CHO cells, the Gβγ inhibitor M119K was used. M119K binds to Gβγ with high affinity and *in vitro* studies demonstrate it inhibits Gβγ function (Bonacci et al., 2006; Kirui et al., 2010) Gβγ subunits can directly activate GIRK channels, and reassociation with Gα subunit terminates this signaling (Lin & Smrcka, 2011; Petit-Jacques, Sui, & Logothetis, 1999). In mOTR and hOTR CHO cells, pretreatment with M119K did not produce a statistically significantly reduction in Leu^8-OT-induced membrane hyperpolarization (Supplementary Figure 6; Supplementary Table 2). Together, these data suggest that in mOTR-expressing cells, but not hOTR CHO cells, Leu^8-OT modulation of membrane potential is partially mediated by GIRK channels, but a role for Gβγ-dependent signaling was not established.

Molecular Pharmacology Fast Forward. Published on February 9, 2019 as DOI: 10.1124/mol.118.114744
This article has not been copyedited and formatted. The final version may differ from this version.

Given that Pro^8-OT-induced changes in membrane potential were insensitive to PTX and Leu^8-OT-induced changes were only partially sensitive in mOTR-expressing cells, we next considered the possibility that OT peptide-induced hyperpolarization may involve coupling to G_q with activation of phospholipase C (PLCβ) and calcium-dependent K^+ channel activation. To explore the role of Ca^{2+}-activated K^+ channels in OT-analog induced changes in membrane potential, we used a pharmacological approach with compounds that discriminate between subtypes of Ca^{2+}-activated K^+ channels. To assess the role of SK_{Ca} channels in OT-mediated membrane hyperpolarization in mOTR and hOTR cells, cells were pretreated with the SK_{Ca}-selective blocker apamin. Molecular modeling and mutational studies suggest apamin functions to block SK_{Ca} channels through an allosteric mechanism rather than a classical pore block (Lamy et al., 2010). In mOTR and hOTR CHO cells, apamin produced very modest inhibition of Leu^8-OT -induced changes, 16.4% and 6.6%, respectively (Figure 4A,C; Supplementary Figure 7A, 8A), and did not affect Pro^8-OT-induced changes in membrane potential (Figure 4B,D; Supplementary Figure 7B, 8B). To confirm that OT-analog vehicle DMSO (0.02%) and apamin solvent acetic acid (5 μM) did not affect membrane hyperpolarization, additional controls were performed. Neither DMSO nor acetic acid vehicles alone affected membrane potential in mOTR and hOTR expressing cells (Supplementary Figure 9). These data indicate that the acetic acid vehicle did not substantially affect membrane hyperpolarization and that SK_{Ca} channels provide minimal contribution to OT analog induced changes in membrane potential in either mOTR or hOTR expressing CHO cells.

Molecular Pharmacology Fast Forward. Published on February 9, 2019 as DOI: 10.1124/mol.118.114744
This article has not been copyedited and formatted. The final version may differ from this version.

Charybdotoxin exhibits blocking effects on both IK_{Ca} and BK_{Ca} (Anderson et al., 1988; Ishii et al., 1997; MacKinnon & Miller, 1988; Qiu et al., 2009). Charybdotoxin binds to the BK_{Ca} channel in either the open or closed conformation and dissociation from the BK_{Ca} channel is voltage-dependent (MacKinnon & Miller, 1988), In mOTR CHO cells, charybdotoxin did not affect changes in membrane potential produced by either Leu^8-OT (Figure 4A; Supplementary Figure 7C) or Pro^8-OT (Figure 4B; Supplementary Figure 7D); however, in hOTR CHO cells charybdotoxin modestly reduced Leu^8-OT- and Pro^8-OT-induced hyperpolarization by 17.0% (Figure 4C; Supplementary Figure 8C) and 24.3% (Figure 4D; Supplementary Figure 8D) respectively. These results suggested that IK_{Ca} and/or BK_{Ca} channels may partially contribute to OT-mediated changes in membrane potential. To further assess the role of BK_{Ca} channels mOTR and hOTR cells were pretreated with the BK_{Ca} blocker paxilline. Paxilline produces inhibition by stabilizing the BK_{Ca} channels in the closed conformation (Y. Zhou & Lingle, 2014). In mOTR CHO cells paxilline did not affect Leu^8-OT-induced changes in membrane potential (Figure 4A; Supplementary Figure 7C), whereas the Pro^8-OT response was reduced by 40.5% (Figure 4B; Supplementary Figure 7D). In hOTR CHO cells, paxilline modestly inhibited hyperpolarization by both Leu^8-OT (20.6%) (Figure 4C; Supplementary Figure 8C) and Pro^8-OT (26.5%) (Figure 4D; Supplementary Figure 8D), suggesting that BK_{Ca} channels do contribute to OT-mediated changes in membrane potential by hOTR. To confirm the involvement BK_{Ca} channels in hyperpolarization of mOTR and hOTR CHO cells we next used the BK_{Ca} activator NS-1619. In mOTR and hOTR CHO cells, paxilline inhibited the NS-1619-induced membrane hyperpolarization in a concentration-dependent manner with a 30 μM paxilline concentration inhibiting the

Molecular Pharmacology Fast Forward. Published on February 9, 2019 as DOI: 10.1124/mol.118.114744
This article has not been copyedited and formatted. The final version may differ from this version.

response by 77.8% and 79.0% respectively (Supplementary Figure 10A-B, E-F), confirming a role for BK_{Ca} channels in the regulation of CHO cell membrane potential.

TRAM-34 is an IK_{Ca} K^+ channel blocker that specifically blocks $K_{Ca}3.1$ by occupying the site that K^+ binds to before entering the selectivity filter (Nguyen et al., 2017). TRAM-34 produced the most robust inhibition of OT-mediated changes in membrane potential. In mOTR CHO cells TRAM-34 inhibited the Leu^8-OT response by 59.2% (Figure 4A; Supplementary Figure 7E) and the Pro^8-OT response by 72.9% (Figure 4B; Supplementary Figure 7F). Similarly, in hOTR CHO cells TRAM-34 inhibited Leu^8-OT by 59.2% (Figure 4C; Supplementary Figure 8E) and Pro^8-OT by 58.9% (Figure 4D; Supplementary Figure 8F). To confirm participation of $K_{Ca}3.1$ channels in the regulation of membrane potential in mOTR and hOTR expressing cells, we next challenged cells with the $K_{Ca}3.1$ activator SKA-31. In mOTR and hOTR CHO cells, TRAM-34 inhibited SKA-31-induced membrane hyperpolarization in a concentration-dependent manner with 300 nM inhibiting the response by 73.4% and 91.5% respectively (Supplementary Figure 10C-D, G-H). These data document an important role for $K_{Ca}3.1$ as a mediator of the response to OTR driven Ca^{2+}-dependent hyperpolarization in mOTR and hOTR expressing CHO cells. To demonstrate the combined contribution of BK_{Ca} and $K_{Ca}3.1$ channels in the observed OT-mediated changes in membrane potential, cells were pretreated with both paxilline and TRAM-34. In mOTR and hOTR CHO cells the combined exposure of paxilline and TRAM-34 inhibited both Leu^8-OT and Pro^8-OT induced hyperpolarization by approximately 85% (Figure 4; Supplementary Figure 7G-H, 8G-H) indicating an additive effect. These data

Molecular Pharmacology Fast Forward. Published on February 9, 2019 as DOI: 10.1124/mol.118.114744
This article has not been copyedited and formatted. The final version may differ from this version.

confirm that BK_{Ca} and IK_{Ca} channels are largely responsible for OT-induced changes in membrane potential.

To directly assess the role of calcium in OT-mediated membrane hyperpolarization, cells were pretreated with the intracellular calcium chelator BAPTA-AM. In both mOTR and hOTR CHO cells, BAPTA-AM exposure blocked hyperpolarization of membrane potential with either Leu^8-OT or Pro^8-OT (Supplementary Figure 11A-B; E-F). Interestingly, in BAPTA-AM treated hOTR CHO cells, a Leu^8-OT-induced depolarization was observed, (Supplementary Figure 11E) indicating a possible dual modulation of K^+ channel currents by the OTR (Gravati et al., 2010).

We next confirmed the role of intracellular calcium stores in OT-mediated changes in membrane potential by pretreating cells with thapsigargin and measuring membrane potential responses to OT analogs in mOTR and hOTR CHO cells. As expected, pretreatment with thapsigargin eliminated hyperpolarization produced by either Leu^8-OT (Supplementary Figure 11C, G) or Pro^8-OT (Supplementary Figure 11D, H). Interestingly, in thapsigargin pretreated hOTR CHO cells, Leu^8-OT and Pro^8-OT both produced a depolarization response (Supplementary Figure 11G-H) again indicating potential dual modulation of currents by the hOTR.

DISCUSSION

Previous studies demonstrated promiscuous activation of various G-proteins by OT peptides in a variety of cell types (Busnelli et al., 2016; Busnelli et al., 2012; Gravati et al., 2010; Parreiras-e-Silva et al., 2017; Phaneuf et al., 1993; Reversi et al., 2005). In

Molecular Pharmacology Fast Forward. Published on February 9, 2019 as DOI: 10.1124/mol.118.114744
This article has not been copyedited and formatted. The final version may differ from this version.

this study we compared a natural variation in OT ligands in mOTR and hOTR expressing CHO cells to assess downstream activation of G-protein signaling pathways. Our findings initially confirmed that at both the mOTR and hOTR Leu^8-OT and Pro^8-OT activated G_q signaling in a concentration-dependent manner resulting in an increase intracellular calcium concentration. Notably, in mOTR CHO cells the cognate ligand Pro^8-OT was more efficacious than Leu^8-OT which may reflect ligand-receptor co-evolutionary changes observed in NWMs (Ren et al., 2015). Alignment using the National Center for Biotechnology Information (NCBI) basic local alignment search tool (BLAST) indicates human and marmoset (*Callithrix jacchus*) OTR are 94% conserved (Boratyn et al., 2012). OT ligands interact with the three-dimensional environment of the extracellular region and transmembrane domains. Amino acid changes are considered radical or conservative based on the magnitude of their physiochemical differences. There are 20 amino acid changes between human and marmoset OTR, six of which are located in the extracellular and transmembrane regions (Supplementary table 5; Ren et al., 2015), that may affect ligand binding. The increased efficacy observed with Pro^8-OT in mOTR CHO cells may contribute to sociobehavioral responses in marmosets. In contrast to the superior efficacy of Pro^8-OT in the calcium mobilization assay at the mOTR, no significant differences in efficacy were observed between Pro^8-OT and Leu^8-OT using the same assay in hOTR CHO cells. Similarly, no significant differences in the potency of either Leu^8-OT or Pro^8-OT were observed in the Ca^{2+} mobilization assay in mOTR and hOTR CHO cells. The observed EC_{50} values were consistent with those found previously in hOTR expressing cell lines (Busnelli et al., 2012; Parreiras-e-Silva et al., 2017), and comparable to results from hOTR expressing HEK cells where Leu^8-

Molecular Pharmacology Fast Forward. Published on February 9, 2019 as DOI: 10.1124/mol.118.114744
This article has not been copyedited and formatted. The final version may differ from this version.

OT, Pro^8-OT, and Val^3- Pro^8-OT function as full agonists at a G_q signaling pathway (Parreiras-e-Silva et al., 2017). The results of these previous studies with hOTR were extended in the present investigation by comparing mOTR and hOTR signaling responses.

Given a previous report that Leu^8-OT exerts a dual modulation of inward rectifier K^+ currents in olfactory neuronal cells (Gravati et al, 2010), we next assessed the ability of OT ligand to trigger a hyperpolarization response. G protein-gated inwardly rectifying potassium (GIRK) channels are regulators of cellular excitability, and stimulation of a variety G-protein-coupled receptors (GPCRs) that couple to $G_{i/o}$ G proteins, such as the μ-opioid receptor, activate GIRK channels via G protein Gβγ subunits (Rifkin, Moss, & Slesinger, 2017). Both OT-ligands induced membrane hyperpolarization in mOTR and hOTR expressing cells in a concentration-dependent manner. The membrane hyperpolarizing responses displayed significant OT peptide-specific differences in potency. In both mOTR and hOTR expressing cells Leu^8-OT was approximately 100-fold more potent than Pro^8-OT in inducing membrane hyperpolarization.

PTX inhibits its G_α protein substrate from coupling to receptors, thus blocking $G_{i/o}$-mediated responses including membrane hyperpolarization mediated by GIRK channels. The efficacy of Leu^8-OT in the FMP Blue assay was only modestly reduced by PTX in mOTR CHO cells. This suggested a minor $G_{i/o}$ and GIRK contribution to Leu^8-OT-induced hyperpolarization of membrane potential. In contrast to the partial sensitivity of Leu^8-OT, the Pro^8-OT-induced hyperpolarization response was completely insensitive to PTX in both mOTR and hOTR expressing CHO cells, demonstrating a bias against G_i activation. This pattern of Leu^8-OT and Pro^8-OT producing primary coupling of OTRs to

Molecular Pharmacology Fast Forward. Published on February 9, 2019 as DOI: 10.1124/mol.118.114744
This article has not been copyedited and formatted. The final version may differ from this version.

G_q, with minor activation of G_i by Leu^8-OT is consistent with previous reports for these peptides in human OTR expressing HEK293 cells (Parreiras-e-Silva et al., 2017). At the hOTR Leu^8-OT has been shown to produce a robust internalization, while the response to Pro^8-OT was modest (Parreiras-e-Silva et al., 2017).

OT has also previously been shown to exert a dual action in olfactory GN11 cells both stimulating and inhibiting K^+ conductances belonging to the inward rectifier (IR) family of K^+ channels (Gravati et al., 2010). The OT-mediated IR current inhibition was mediated by a PTX-resistant G protein, presumably of the $G_{q/11}$ subtype, and by PLC activation, whereas the activation of a K^+ conductance was mediated by a PTX-sensitive $G_{i/o}$ (Gravati et al., 2010). These differences in G protein subtype regulation of K^+ conductances observed previously in the GN11 cell line underscore the importance of cellular context in measurements of signaling pathways. The partial PTX sensitivity observed at the mOTR with Leu^8-OT, but not Pro^8-OT, appears to represent an agonist functional selectivity where the two OT ligands activate a single receptor but produce distinct signaling outcomes (Rankovic, Brust, & Bohn, 2016).

A variety of hormones and neurotransmitters acting at G-protein coupled receptors (GPCR) are capable of producing $[Ca^{2+}]_i$ elevation typically mediated by Ca^{2+} release from endoplasmic reticulum via the Gq/phosphoinositide-phospholipase C (Gq/PI-PLC) pathway. This G_q-siqnaling pathway affords another potential mechanism for hyperpolarizing responses through activation of Ca^{2+}-dependent potassium channels. A role for Ca^{2+}-activated K^+ channels in the hyperpolarization responses observed in mOTR and hOTR expressing CHO cells was therefore assessed using BK_{Ca} ($K_{Ca}1.1$), IK_{Ca} ($K_{Ca}3.1$) and SK_{Ca} channel blockers. Paxilline selectively blocks

Molecular Pharmacology Fast Forward. Published on February 9, 2019 as DOI: 10.1124/mol.118.114744
This article has not been copyedited and formatted. The final version may differ from this version.

BK_{Ca} channels, and pretreatment with this inhibitor resulted in a significant reduction in the hyperpolarization response observed with Pro^8-OT in mOTR cells, and the response to both Leu^8-OT and Pro^8-OT in hOTR expressing cells. Paxilline also inhibited the hyperpolarizing response to the BK_{Ca} channel opener NS-1619 in both mOTR and hOTR CHO cells, further supporting a role for a BK_{Ca} channel contribution to the observed membrane hyperpolarization. These results agree with those of an earlier report demonstrating that Leu^8-OT hyperpolarized myenteric intrinsic primary afferent neurons by activating BK_{Ca} channels via the OTR-PLC-IP3- Ca^{2+} signaling pathway (Che et al., 2012).

TRAM-34 inhibited between 58-73% of the hyperpolarizing responses to both OT-ligands, suggesting $K_{Ca}3.1$ is largely responsible for membrane hyperpolarization produced by OT peptides in mOTR and hOTR expressing CHO cells. TRAM-34 also inhibited the hyperpolarizing response to $K_{Ca}3.1$ opener SKA-31, further demonstrating the involvement of $K_{Ca}3.1$ in observed membrane hyperpolarization. The critical role of $[Ca^{2+}]_i$ elevation in the hyperpolarization was demonstrated using BAPTA-AM to chelate intracellular Ca^{2+} (Strayer et al., 1999). Pretreatment with BAPTA-AM eliminated membrane hyperpolarization in response to both OT analogs in mOTR and hOTR cells. Similarly, passive depletion of endoplasmic reticulum Ca^{2+} stores by the endoplasmic reticulum Ca^{2+}-ATPase inhibitor, thapsigargin (Dravid & Murray, 2004; Quynh Doan & Christensen, 2015) also inhibited OT-induced membrane hyperpolarization produced by both OT analogs in both cell lines. These data confirm that the observed OT ligand induced membrane hyperpolarization in mOTR and hOTR expressing CHO cells was

Molecular Pharmacology Fast Forward. Published on February 9, 2019 as DOI: 10.1124/mol.118.114744
This article has not been copyedited and formatted. The final version may differ from this version.

primarily mediated by intracellular Ca^{2+} mobilization with subsequent activation of Ca^{2+}-dependent K^+ channels, including $K_{Ca}3.1$.

OT is a fundamental mediator of sociobehavioral processes including social cognition (Crespi, 2016), interpersonal trust (Baumgartner et al., 2008; Kosfeld et al., 2005), anxiety (Missig et al., 2010), and stress response (Cavanaugh et al., 2016; Light et al., 2000), generating interest in OT as potential therapeutic mediator of sociobehavioral deficits in conditions such as autism spectrum disorder (Anagnostou et al., 2012; Andari et al., 2010), post-traumatic stress disorder (Frijling, 2017; Sack et al., 2017), and schizophrenia (Brambilla et al., 2016; Pedersen et al., 2011). One major challenge is connecting pharmacologic signatures to sociobehavioral processes. Identification of the mechanisms by which OT analogs affect OTR-mediated signaling is crucial to translating signaling activation at the cellular level to effects of OT ligands on social behaviors. In clinical trials for sociobehavioral deficits, intranasal OT is used because peripheral administration does not cross the blood-brain barrier (Born et al., 2002). Intranasal OT appears to be safe and well-tolerated (Anagnostou et al., 2012) and imaging evidence suggests OT induces increased activity in the 'social brain' (Bethlehem, van Honk, Auyeung, & Baron-Cohen, 2013). However, clinical trials for OT treatment of sociobehaivioral deficits with various dosing schedules (single vs. multiple) and routes (IV vs. intranasal) have shown mixed results (Alvares, Quintana, & Whitehouse, 2017) suggesting that greater understanding of OT triggered signaling pathways downstream of the OTR could facilitate interpretation of sociobehavioral effects leading to more refined therapeutic targeting.

The present results show that Leu^8-OT and Pro^8-OT display functionally distinct responses when activating either the mOTR or hOTR. These distinct characteristics included peptide potency and efficacy, and G-protein subtype coupling. Pro^8-OT was shown to be more efficacious than Leu^8-OT in activating the G_q Ca^{2+} mobilization assay in mOTR cells. Uniquely, Leu^8-OT was much more potent than Pro^8-OT in producing a hyperpolarization in both mOTR and hOTR. A final salient difference in the observed pharmacologic signatures of the two peptides was that the Pro^8-OT-induced hyperpolarization responses in both mOTR and hOTR were PTX insensitive whereas the response to Leu^8-OT in mOTR was partially sensitive. Further functional characterization of OT analogs may therefore provide insight into the structural requirements for functionally selective or biased agonists that open new possibilities for drug discovery and the advancement of OT-mediated therapeutics.

Molecular Pharmacology Fast Forward. Published on February 9, 2019 as DOI: 10.1124/mol.118.114744
This article has not been copyedited and formatted. The final version may differ from this version.

AKNOWLEDGMENTS

We would like to thank Dr. Myron Toews for his input during the planning of this project and Dr. Jack Taylor and Ms. Bridget Sefranek for their careful reading of the manuscript.

Molecular Pharmacology Fast Forward. Published on February 9, 2019 as DOI: 10.1124/mol.118.114744
This article has not been copyedited and formatted. The final version may differ from this version.

AUTHORSHIP CONTRIBUTIONS

Participated in research design: Murray, Pierce, Mehrotra

Conducted experiments: Pierce, Mehrotra, Mustoe

Performed data analysis: Pierce, Mehrotra, Mustoe

Wrote or contributed to the writing of the manuscript: Murray, Pierce, Mehrotra, Mustoe, French

REFERENCES

Alvares, G. A., Quintana, D. S., & Whitehouse, A. J. (2017). Beyond the hype and hope: Critical considerations for intranasal oxytocin research in autism spectrum disorder. *Autism Res, 10*(1), 25-41. doi:10.1002/aur.1692

Anagnostou, E., Soorya, L., Chaplin, W., Bartz, J., Halpern, D., Wasserman, S., . . . Hollander, E. (2012). Intranasal oxytocin versus placebo in the treatment of adults with autism spectrum disorders: a randomized controlled trial. *Mol Autism, 3*(1), 16. doi:10.1186/2040-2392-3-16

Andari, E., Duhamel, J. R., Zalla, T., Herbrecht, E., Leboyer, M., & Sirigu, A. (2010). Promoting social behavior with oxytocin in high-functioning autism spectrum disorders. *Proc Natl Acad Sci U S A, 107*(9), 4389-4394. doi:10.1073/pnas.0910249107

Anderson, A. J., Harvey, A. L., Rowan, E. G., & Strong, P. N. (1988). Effects of charybdotoxin, a blocker of Ca2+-activated K+ channels, on motor nerve terminals. *Br J Pharmacol, 95*(4), 1329-1335.

Baumgartner, T., Heinrichs, M., Vonlanthen, A., Fischbacher, U., & Fehr, E. (2008). Oxytocin shapes the neural circuitry of trust and trust adaptation in humans. *Neuron, 58*(4), 639-650. doi:10.1016/j.neuron.2008.04.009

Baxter, D. F., Kirk, M., Garcia, A. F., Raimondi, A., Holmqvist, M. H., Flint, K. K., . . . Xie, Y. (2002). A novel membrane potential-sensitive fluorescent dye improves cell-based assays for ion channels. *J Biomol Screen, 7*(1), 79-85. doi:10.1177/108705710200700110

Bethlehem, R. A., van Honk, J., Auyeung, B., & Baron-Cohen, S. (2013). Oxytocin, brain physiology, and functional connectivity: a review of intranasal oxytocin fMRI studies. *Psychoneuroendocrinology, 38*(7), 962-974. doi:10.1016/j.psyneuen.2012.10.011

Blatz, A. L., & Magleby, K. L. (1986). Single apamin-blocked Ca-activated K+ channels of small conductance in cultured rat skeletal muscle. *Nature, 323*(6090), 718-720. doi:10.1038/323718a0

Bonacci, T. M., Mathews, J. L., Yuan, C., Lehmann, D. M., Malik, S., Wu, D., . . . Smrcka, A. V. (2006). Differential targeting of Gbetagamma-subunit signaling with small molecules. *Science, 312*(5772), 443-446. doi:10.1126/science.1120378

Boratyn, G. M., Schaffer, A. A., Agarwala, R., Altschul, S. F., Lipman, D. J., & Madden, T. L. (2012). Domain enhanced lookup time accelerated BLAST. *Biol Direct, 7*, 12. doi:10.1186/1745-6150-7-12

Born, J., Lange, T., Kern, W., McGregor, G. P., Bickel, U., & Fehm, H. L. (2002). Sniffing neuropeptides: a transnasal approach to the human brain. *Nat Neurosci, 5*(6), 514-516. doi:10.1038/nn849

Brambilla, M., Cotelli, M., Manenti, R., Dagani, J., Sisti, D., Rocchi, M., . . . de Girolamo, G. (2016). Oxytocin to modulate emotional processing in schizophrenia: A randomized, double-blind, cross-over clinical trial. *Eur Neuropsychopharmacol, 26*(10), 1619-1628. doi:10.1016/j.euroneuro.2016.08.001

Busnelli, M., Kleinau, G., Muttenthaler, M., Stoev, S., Manning, M., Bibic, L., . . . Chini, B. (2016). Design and Characterization of Superpotent Bivalent Ligands Targeting Oxytocin

Receptor Dimers via a Channel-Like Structure. *J Med Chem, 59*(15), 7152-7166. doi:10.1021/acs.jmedchem.6b00564

Busnelli, M., Sauliere, A., Manning, M., Bouvier, M., Gales, C., & Chini, B. (2012). Functional selective oxytocin-derived agonists discriminate between individual G protein family subtypes. *J Biol Chem, 287*(6), 3617-3629. doi:10.1074/jbc.M111.277178

Cavanaugh, J., Carp, S. B., Rock, C. M., & French, J. A. (2016). Oxytocin modulates behavioral and physiological responses to a stressor in marmoset monkeys. *Psychoneuroendocrinology, 66*, 22-30. doi:10.1016/j.psyneuen.2015.12.027

Che, T., Sun, H., Li, J., Yu, X., Zhu, D., Xue, B., . . . Liu, C. (2012). Oxytocin hyperpolarizes cultured duodenum myenteric intrinsic primary afferent neurons by opening BK(Ca) channels through IP(3) pathway. *J Neurochem, 121*(4), 516-525. doi:10.1111/j.1471-4159.2012.07702.x

Chini, B., Mouillac, B., Ala, Y., Balestre, M. N., Trumpp-Kallmeyer, S., Hoflack, J., . . . et al. (1995). Tyr115 is the key residue for determining agonist selectivity in the V1a vasopressin receptor. *EMBO J, 14*(10), 2176-2182.

Chini, B., Mouillac, B., Balestre, M. N., Trumpp-Kallmeyer, S., Hoflack, J., Hibert, M., . . . Barberis, C. (1996). Two aromatic residues regulate the response of the human oxytocin receptor to the partial agonist arginine vasopressin. *FEBS Lett, 397*(2-3), 201-206.

Christophersen, P., & Wulff, H. (2015). Pharmacological gating modulation of small- and intermediate-conductance Ca(2+)-activated K(+) channels (KCa2.x and KCa3.1). *Channels (Austin), 9*(6), 336-343. doi:10.1080/19336950.2015.1071748

Crespi, B. J. (2016). Oxytocin, testosterone, and human social cognition. *Biol Rev Camb Philos Soc, 91*(2), 390-408. doi:10.1111/brv.12175

Dravid, S. M., & Murray, T. F. (2004). Spontaneous synchronized calcium oscillations in neocortical neurons in the presence of physiological [Mg(2+)]: involvement of AMPA/kainate and metabotropic glutamate receptors. *Brain Res, 1006*(1), 8-17. doi:10.1016/j.brainres.2004.01.059

Edwards, G., Niederste-Hollenberg, A., Schneider, J., Noack, T., & Weston, A. H. (1994). Ion channel modulation by NS 1619, the putative BKCa channel opener, in vascular smooth muscle. *Br J Pharmacol, 113*(4), 1538-1547.

French, J. A., Taylor, J. H., Mustoe, A. C., & Cavanaugh, J. (2016). Neuropeptide diversity and the regulation of social behavior in New World primates. *Front Neuroendocrinol, 42*, 18-39. doi:10.1016/j.yfrne.2016.03.004

Frijling, J. L. (2017). Preventing PTSD with oxytocin: effects of oxytocin administration on fear neurocircuitry and PTSD symptom development in recently trauma-exposed individuals. *Eur J Psychotraumatol, 8*(1), 1302652. doi:10.1080/20008198.2017.1302652

Geisler, I., & Chmielewski, J. (2009). Cationic amphiphilic polyproline helices: side-chain variations and cell-specific internalization. *Chem Biol Drug Des, 73*(1), 39-45. doi:10.1111/j.1747-0285.2008.00759.x

Gimpl, G., & Fahrenholz, F. (2001). The oxytocin receptor system: structure, function, and regulation. *Physiol Rev, 81*(2), 629-683.

Gravati, M., Busnelli, M., Bulgheroni, E., Reversi, A., Spaiardi, P., Parenti, M., . . . Chini, B. (2010). Dual modulation of inward rectifier potassium currents in olfactory neuronal cells by promiscuous G protein coupling of the oxytocin receptor. *J Neurochem, 114*(5), 1424-1435. doi:10.1111/j.1471-4159.2010.06861.x

Guastella, A. J., & Hickie, I. B. (2016). Oxytocin Treatment, Circuitry, and Autism: A Critical Review of the Literature Placing Oxytocin Into the Autism Context. *Biol Psychiatry, 79*(3), 234-242. doi:10.1016/j.biopsych.2015.06.028

Insel, T., Cuthbert, B., Garvey, M., Heinssen, R., Pine, D. S., Quinn, K., . . . Wang, P. (2010). Research domain criteria (RDoC): toward a new classification framework for research on mental disorders. *Am J Psychiatry, 167*(7), 748-751. doi:10.1176/appi.ajp.2010.09091379

Ishii, T. M., Silvia, C., Hirschberg, B., Bond, C. T., Adelman, J. P., & Maylie, J. (1997). A human intermediate conductance calcium-activated potassium channel. *Proc Natl Acad Sci U S A, 94*(21), 11651-11656.

Johnson, Z. V., & Young, L. J. (2015). Neurobiological mechanisms of social attachment and pair bonding. *Curr Opin Behav Sci, 3*, 38-44. doi:10.1016/j.cobeha.2015.01.009

Kirui, J. K., Xie, Y., Wolff, D. W., Jiang, H., Abel, P. W., & Tu, Y. (2010). Gbetagamma signaling promotes breast cancer cell migration and invasion. *J Pharmacol Exp Ther, 333*(2), 393-403. doi:10.1124/jpet.109.164814

Kosfeld, M., Heinrichs, M., Zak, P. J., Fischbacher, U., & Fehr, E. (2005). Oxytocin increases trust in humans. *Nature, 435*(7042), 673-676. doi:10.1038/nature03701

Lamy, C., Goodchild, S. J., Weatherall, K. L., Jane, D. E., Liegeois, J. F., Seutin, V., & Marrion, N. V. (2010). Allosteric block of KCa2 channels by apamin. *J Biol Chem, 285*(35), 27067-27077. doi:10.1074/jbc.M110.110072

Lee, A. G., Cool, D. R., Grunwald, W. C., Jr., Neal, D. E., Buckmaster, C. L., Cheng, M. Y., . . . Parker, K. J. (2011). A novel form of oxytocin in New World monkeys. *Biol Lett, 7*(4), 584-587. doi:10.1098/rsbl.2011.0107

Lee, K., Rowe, I. C., & Ashford, M. L. (1995). NS 1619 activates BKCa channel activity in rat cortical neurones. *Eur J Pharmacol, 280*(2), 215-219.

Light, K. C., Smith, T. E., Johns, J. M., Brownley, K. A., Hofheimer, J. A., & Amico, J. A. (2000). Oxytocin responsivity in mothers of infants: a preliminary study of relationships with blood pressure during laboratory stress and normal ambulatory activity. *Health Psychol, 19*(6), 560-567.

Lin, Y., & Smrcka, A. V. (2011). Understanding molecular recognition by G protein betagamma subunits on the path to pharmacological targeting. *Mol Pharmacol, 80*(4), 551-557. doi:10.1124/mol.111.073072

Ludwig, M., & Leng, G. (2006). Dendritic peptide release and peptide-dependent behaviours. *Nat Rev Neurosci, 7*(2), 126-136. doi:10.1038/nrn1845

MacKinnon, R., & Miller, C. (1988). Mechanism of charybdotoxin block of the high-conductance, Ca2+-activated K+ channel. *J Gen Physiol, 91*(3), 335-349.

Manning, M., Stoev, S., Chini, B., Durroux, T., Mouillac, B., & Guillon, G. (2008). Peptide and non-peptide agonists and antagonists for the vasopressin and oxytocin V1a, V1b, V2 and OT receptors: research tools and potential therapeutic agents. *Prog Brain Res, 170*, 473-512. doi:10.1016/S0079-6123(08)00437-8

Missig, G., Ayers, L. W., Schulkin, J., & Rosen, J. B. (2010). Oxytocin reduces background anxiety in a fear-potentiated startle paradigm. *Neuropsychopharmacology, 35*(13), 2607-2616. doi:10.1038/npp.2010.155

Murray, T. F. Siebenaller., J.F. (1993). Differential Susceptibility of Guanine Nucleotide- binding Proteins to Pertussis Toxin-catalyzed ADP- ribosylation in Brain Membranes of Two Congeneric Marine Fishes. *Bio. Bull.*(185), 346-354.

Murthy, K. S., & Makhlouf, G. M. (1996). Opioid mu, delta, and kappa receptor-induced activation of phospholipase C-beta 3 and inhibition of adenylyl cyclase is mediated by Gi2 and G(o) in smooth muscle. *Mol Pharmacol, 50*(4), 870-877.

Nguyen, H. M., Singh, V., Pressly, B., Jenkins, D. P., Wulff, H., & Yarov-Yarovoy, V. (2017). Structural Insights into the Atomistic Mechanisms of Action of Small Molecule Inhibitors Targeting the KCa3.1 Channel Pore. *Mol Pharmacol, 91*(4), 392-402. doi:10.1124/mol.116.108068

Parker, K. J., Oztan, O., Libove, R. A., Sumiyoshi, R. D., Jackson, L. P., Karhson, D. S., . . . Hardan, A. Y. (2017). Intranasal oxytocin treatment for social deficits and biomarkers of

response in children with autism. *Proc Natl Acad Sci U S A, 114*(30), 8119-8124. doi:10.1073/pnas.1705521114

Parreiras-e-Silva L. T., Vargas-Pinilla, P., Duarte, D. A., Longo, D., Espinoza Pardo, G. V., Dulor Finkler, A., . . . Bortolini, M. C. (2017). Functional New World monkey oxytocin forms elicit an altered signaling profile and promotes parental care in rats. *Proc Natl Acad Sci U S A, 114*(34), 9044-9049. doi:10.1073/pnas.1711687114

Pedersen, C. A., Gibson, C. M., Rau, S. W., Salimi, K., Smedley, K. L., Casey, R. L., . . . Penn, D. L. (2011). Intranasal oxytocin reduces psychotic symptoms and improves Theory of Mind and social perception in schizophrenia. *Schizophr Res, 132*(1), 50-53. doi:10.1016/j.schres.2011.07.027

Petit-Jacques, J., Sui, J. L., & Logothetis, D. E. (1999). Synergistic activation of G protein-gated inwardly rectifying potassium channels by the betagamma subunits of G proteins and Na(+) and Mg(2+) ions. *J Gen Physiol, 114*(5), 673-684.

Phaneuf, S., Europe-Finner, G. N., Varney, M., MacKenzie, I. Z., Watson, S. P., & Lopez Bernal, A. (1993). Oxytocin-stimulated phosphoinositide hydrolysis in human myometrial cells: involvement of pertussis toxin-sensitive and -insensitive G-proteins. *J Endocrinol, 136*(3), 497-509.

Qiu, S., Yi, H., Liu, H., Cao, Z., Wu, Y., & Li, W. (2009). Molecular Information of charybdotoxin blockade in the large conductance calcium-activated potassium channel. *J Chem Inf Model, 49*(7), 1831-1838. doi:10.1021/ci900025n

Quynh Doan, N. T., & Christensen, S. B. (2015). Thapsigargin, Origin, Chemistry, Structure-Activity Relationships and Prodrug Development. *Curr Pharm Des, 21*(38), 5501-5517.

Rankovic, Z., Brust, T. F., & Bohn, L. M. (2016). Biased agonism: An emerging paradigm in GPCR drug discovery. *Bioorg Med Chem Lett, 26*(2), 241-250. doi:10.1016/j.bmcl.2015.12.024

Ren, D., Lu, G., Moriyama, H., Mustoe, A. C., Harrison, E. B., & French, J. A. (2015). Genetic diversity in oxytocin ligands and receptors in New World monkeys. *PLoS One, 10*(5), e0125775. doi:10.1371/journal.pone.0125775

Reversi, A., Cassoni, P., & Chini, B. (2005). Oxytocin receptor signaling in myoepithelial and cancer cells. *J Mammary Gland Biol Neoplasia, 10*(3), 221-229. doi:10.1007/s10911-005-9583-7

Rifkin, R. A., Moss, S. J., & Slesinger, P. A. (2017). G Protein-Gated Potassium Channels: A Link to Drug Addiction. *Trends Pharmacol Sci, 38*(4), 378-392. doi:10.1016/j.tips.2017.01.007

Ritter, S. L., & Hall, R. A. (2009). Fine-tuning of GPCR activity by receptor-interacting proteins. *Nat Rev Mol Cell Biol, 10*(12), 819-830.

Sack, M., Spieler, D., Wizelman, L., Epple, G., Stich, J., Zaba, M., & Schmidt, U. (2017). Intranasal oxytocin reduces provoked symptoms in female patients with posttraumatic stress disorder despite exerting sympathomimetic and positive chronotropic effects in a randomized controlled trial. *BMC Med, 15*(1), 40. doi:10.1186/s12916-017-0801-0

Sanchez, M., & McManus, O. B. (1996). Paxilline inhibition of the alpha-subunit of the high-conductance calcium-activated potassium channel. *Neuropharmacology, 35*(7), 963-968.

Sankaranarayanan, A., Raman, G., Busch, C., Schultz, T., Zimin, P. I., Hoyer, J., . . . Wulff, H. (2009). Naphtho[1,2-d]thiazol-2-ylamine (SKA-31), a new activator of KCa2 and KCa3.1 potassium channels, potentiates the endothelium-derived hyperpolarizing factor response and lowers blood pressure. *Mol Pharmacol, 75*(2), 281-295. doi:10.1124/mol.108.051425

Sehgal, P., Szalai, P., Olesen, C., Praetorius, H. A., Nissen, P., Christensen, S. B., . . . Moller, J. V. (2017). Inhibition of the sarco/endoplasmic reticulum (ER) Ca(2+)-ATPase by thapsigargin analogs induces cell death via ER Ca(2+) depletion and the unfolded protein response. *J Biol Chem, 292*(48), 19656-19673. doi:10.1074/jbc.M117.796920

Staal, R. G., Khayrullina, T., Zhang, H., Davis, S., Fallon, S. M., Cajina, M., . . . Mller, T. (2017). Inhibition of the potassium channel KCa3.1 by senicapoc reverses tactile allodynia in rats with peripheral nerve injury. *Eur J Pharmacol, 795*, 1-7. doi:10.1016/j.ejphar.2016.11.031

Stoop, R. (2014). Neuromodulation by oxytocin and vasopressin in the central nervous system as a basis for their rapid behavioral effects. *Curr Opin Neurobiol, 29*, 187-193. doi:10.1016/j.conb.2014.09.012

Strayer, D. S., Hoek, J. B., Thomas, A. P., & White, M. K. (1999). Cellular activation by Ca2+ release from stores in the endoplasmic reticulum but not by increased free Ca2+ in the cytosol. *Biochem J, 344 Pt 1*, 39-46.

Sun, X., Hirano, A. A., Brecha, N. C., & Barnes, S. (2017). Calcium-activated BKCa channels govern dynamic membrane depolarizations of horizontal cells in rodent retina. *J Physiol, 595*(13), 4449-4465. doi:10.1113/JP274132

Vargas-Pinilla, P., Paixao-Cortes, V. R., Pare, P., Tovo-Rodrigues, L., Vieira, C. M., Xavier, A., . . . Bortolini, M. C. (2015). Evolutionary pattern in the OXT-OXTR system in primates: coevolution and positive selection footprints. *Proc Natl Acad Sci U S A, 112*(1), 88-93. doi:10.1073/pnas.1419399112

Vergara, C., Latorre, R., Marrion, N. V., & Adelman, J. P. (1998). Calcium-activated potassium channels. *Curr Opin Neurobiol, 8*(3), 321-329.

Wallis, M. (2012). Molecular evolution of the neurohypophysial hormone precursors in mammals: Comparative genomics reveals novel mammalian oxytocin and vasopressin analogues. *Gen Comp Endocrinol, 179*(2), 313-318. doi:10.1016/j.ygcen.2012.07.030

Wang, Y. F., & Hatton, G. I. (2007). Interaction of extracellular signal-regulated protein kinase 1/2 with actin cytoskeleton in supraoptic oxytocin neurons and astrocytes: role in burst firing. *J Neurosci, 27*(50), 13822-13834. doi:10.1523/JNEUROSCI.4119-07.2007

Whiteaker, K. L., Gopalakrishnan, S. M., Groebe, D., Shieh, C. C., Warrior, U., Burns, D. J., . . . Gopalakrishnan, M. (2001). Validation of FLIPR membrane potential dye for high throughput screening of potassium channel modulators. *J Biomol Screen, 6*(5), 305-312. doi:10.1177/108705710100600504

Wulff, H., Miller, M. J., Hansel, W., Grissmer, S., Cahalan, M. D., & Chandy, K. G. (2000). Design of a potent and selective inhibitor of the intermediate-conductance Ca2+-activated K+ channel, IKCa1: a potential immunosuppressant. *Proc Natl Acad Sci U S A, 97*(14), 8151-8156.

Young, L. J., & Barrett, C. E. (2015). Neuroscience. Can oxytocin treat autism? *Science, 347*(6224), 825-826. doi:10.1126/science.aaa8120

Zhou, X. B., Lutz, S., Steffens, F., Korth, M., & Wieland, T. (2007). Oxytocin receptors differentially signal via Gq and Gi proteins in pregnant and nonpregnant rat uterine myocytes: implications for myometrial contractility. *Mol Endocrinol, 21*(3), 740-752. doi:10.1210/me.2006-0220

Zhou, Y., & Lingle, C. J. (2014). Paxilline inhibits BK channels by an almost exclusively closed-channel block mechanism. *J Gen Physiol, 144*(5), 415-440. doi:10.1085/jgp.201411259

Zingg, H. H., & Laporte, S. A. (2003). The oxytocin receptor. *Trends Endocrinol Metab, 14*(5), 222-227.

FOOTNOTES

This work was supported by the National Institutes of Health Eunice Kennedy Shriver National Institute of Child Health and Human Development [Grant R01HD089147].

Pierce, M.L., Mehrotra, S., Toews, M.L., French, J.A., and Murray, T.F., Comparison of Leu^{8}- and Pro^{8}-oxytocin potency, efficacy and functional selectivity at the human and marmoset receptors. Program No. 35.13.2016 Neuroscience Meeting Planner, Society for Neuroscience, Online.

Molecular Pharmacology Fast Forward. Published on February 9, 2019 as DOI: 10.1124/mol.118.114744
This article has not been copyedited and formatted. The final version may differ from this version.

LEGENDS FOR FIGURES

Figure 1. Leu^8-OT and Pro^8-OT induced intracellular calcium mobilization in marmoset oxytocin-receptor expressing (mOTR) expressing or human oxytocin-receptor expressing (hOTR) CHO cells. Leu^8-OT time-response (A) Pro^8-OT time-response (B) and concentration-response relationships (C) in mOTR cells. Leu^8-OT time-response (D) Pro^8-OT time-response (E) and concentration-response relationships (F) in hOTR cells. N=6 experiments (five replicates per concentration per experiment).

Figure 2. Leu^8-OT and Pro^8-OT induced changes in membrane potential in mOTR- or hOTR- expressing CHO cells. Leu^8-OT time-response (A) Pro^8-OT time-response (B) and concentration-response relationships (C) in mOTR cells. Leu^8-OT time-response (D) Pro^8-OT time-response (E) and concentration-response relationships (F) in hOTR cells. N=6 experiments (five replicates per dose per experiment).

Figure 3. Effects of pretreatment with PTX on Leu^8-OT and Pro^8-OT induced changes in membrane potential in mOTR and hOTR-expressing CHO cells. Control Leu^8-OT and PTX-pretreated concentration response relationships (A) and control Pro^8-OT and PTX-pretreated concentration-response relationships (B) in mOTR-expressing cells. Control Leu^8-OT and PTX-pretreated concentration-response relationships (C) and control Pro^8-OT and PTX-pretreated concentration-response relationships (D) in hOTR-expressing cells. Control and PTX-pretreated replicates were run in parallel on the same plates, at the same time and with the same split of cells. N=6 experiments (five replicates per dose per experiment).

Molecular Pharmacology Fast Forward. Published on February 9, 2019 as DOI: 10.1124/mol.118.114744
This article has not been copyedited and formatted. The final version may differ from this version.

Figure 4. Effects of pretreatment with Ca^{2+}-activated K^+ inhibitors on Leu^8-OT or Pro^8-OT induced changes in membrane potential in mOTR and hOTR-expressing CHO cells. Inhibitor fluorescence was normalized to Leu^8-OT or Pro^8-OT-induced membrane hyperpolarization. Area under the curve (negative peaks only) was assessed and a one-way ANOVA was performed with Sidek's multiple comparisons to determine statistical significance. N=3 experiments for each inhibitor (10 replicates per dose per experiment). Raw data (Supplementary Figures 7-8). Adjusted p-values (Supplementary Table 3).

Molecular Pharmacology Fast Forward. Published on February 9, 2019 as DOI: 10.1124/mol.118.114744
This article has not been copyedited and formatted. The final version may differ from this version.

TABLES

Table 1.

		Ligand (nM)		
Line	Parameter	Leu^8-OT	Pro^8-OT	Rank order potency
mOTR	EC_{50}	0.5	0.4	Pro^8-OT = Leu^8-OT
	95% CI	0.3 to 1.0	0.2 to 0.7	
	R^2	0.90	0.92	
hOTR	EC_{50}	0.7	1.6	Leu^8-OT= Pro^8-OT
	95% CI	0.4 to 1.5	0.7 to 3.6	
	R^2	0.87	0.84	

Potency of Leu^8-OT and Pro^8-OT at inducing calcium mobilization in mOTR and hOTR CHO cells.

Molecular Pharmacology Fast Forward. Published on February 9, 2019 as DOI: 10.1124/mol.118.114744
This article has not been copyedited and formatted. The final version may differ from this version.

Table 2.

		Ligand		
Line	Parameter	Leu^8-OT	Pro^8-OT	Rank order potency
mOTR	EC_{50}	11.6 pM	1.1 nM	Leu^8-OT > Pro^8-OT
	95% CI	3.1 to 47.3 pM	0.2 to 5.6 nM	
	R^2	0.71	0.53	
hOTR	EC_{50}	25.6 pM	13.23 nM	Leu^8-OT > Pro^8-OT
	95% CI	4.4 to 150.0 pM	2.4 to 73.6 nM	
	R^2	0.53	0.54	

Potency of Leu^8-OT and Pro^8-OT at inducing membrane hyperpolarization in mOTR and hOTR CHO cells.

Molecular Pharmacology Fast Forward. Published on February 9, 2019 as DOI: 10.1124/mol.118.114744
This article has not been copyedited and formatted. The final version may differ from this version.

FIGURES

Figure 1.

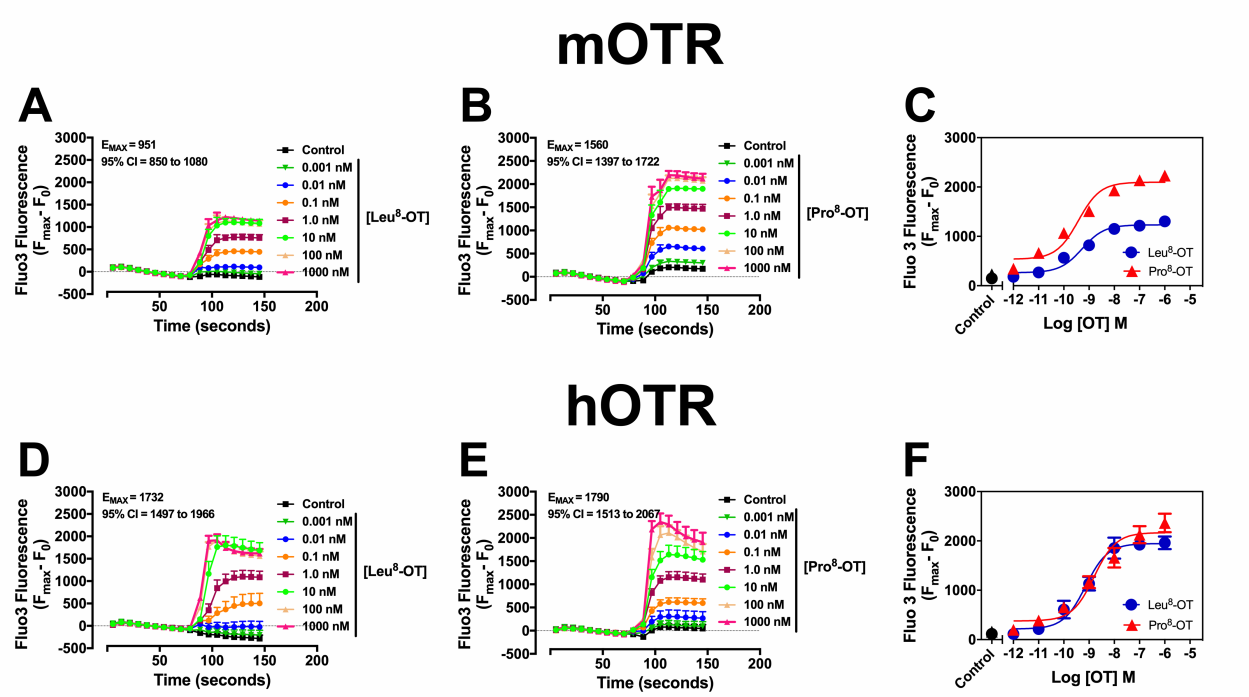

Molecular Pharmacology Fast Forward. Published on February 9, 2019 as DOI: 10.1124/mol.118.114744
This article has not been copyedited and formatted. The final version may differ from this version.

Figure 2.

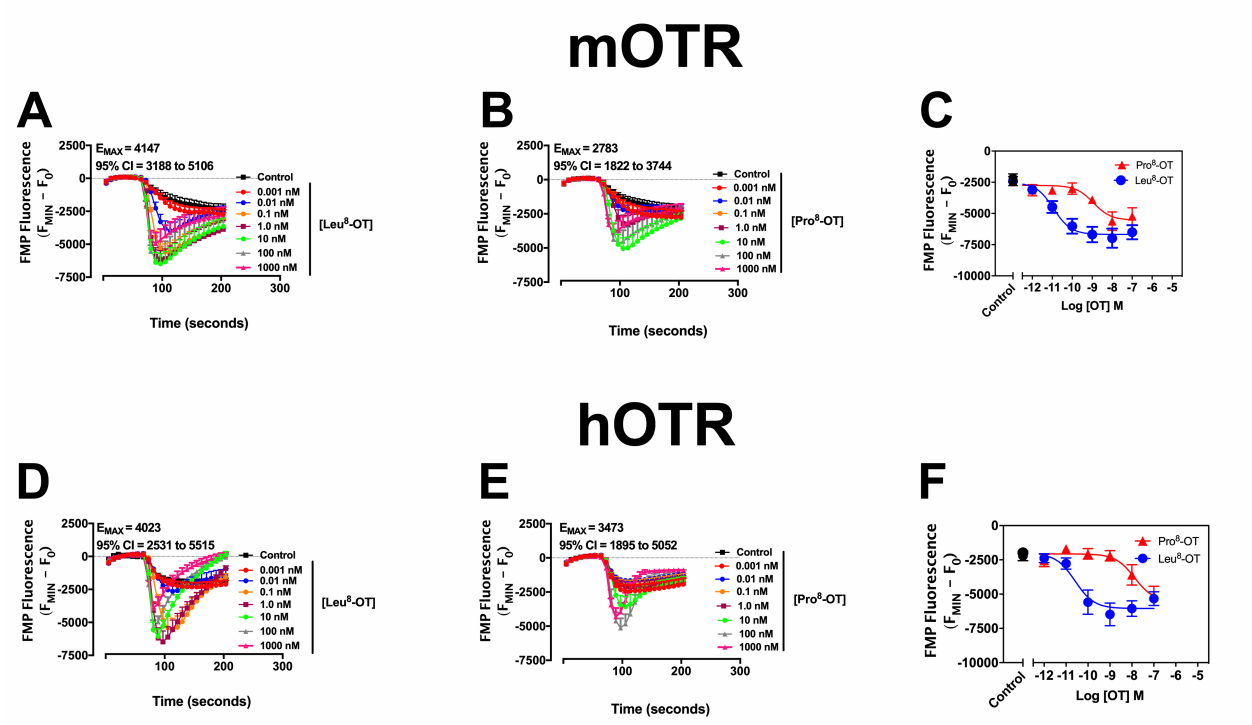

Molecular Pharmacology Fast Forward. Published on February 9, 2019 as DOI: 10.1124/mol.118.114744
This article has not been copyedited and formatted. The final version may differ from this version.

Figure 3.

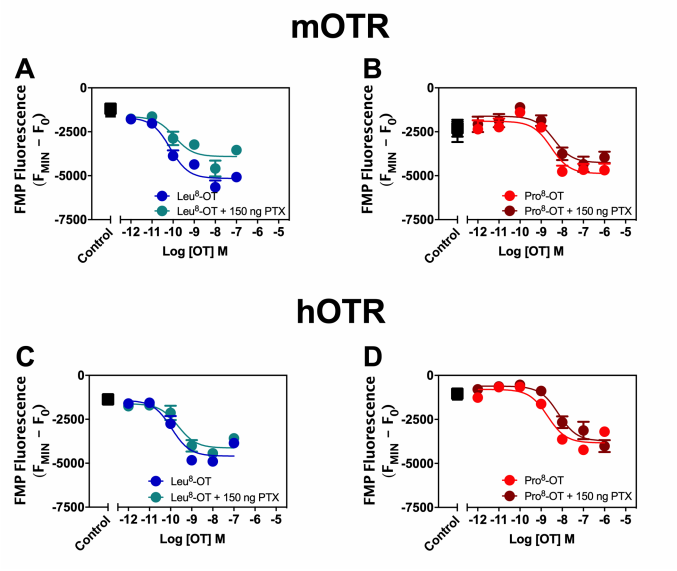

Molecular Pharmacology Fast Forward. Published on February 9, 2019 as DOI: 10.1124/mol.118.114744
This article has not been copyedited and formatted. The final version may differ from this version.

Figure 4.

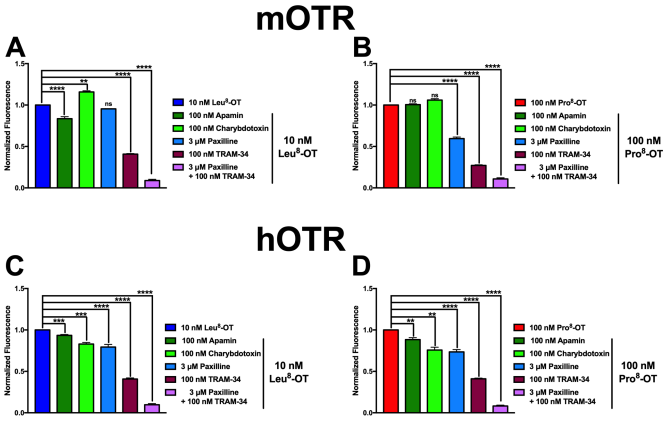

A comparison of the ability of Leu^8- and Pro^8-oxytocin to regulate intracellular Ca^{2+} and Ca^{2+}-activated K^+ channels at human and marmoset oxytocin receptors

Marsha L. Pierce, Suneet Mehrotra, Aaryn C. Mustoe, Jeffrey A. French, Thomas F. Murray

Department of Pharmacology, Creighton University School of Medicine, 2500 California Plaza, Omaha, NE 68178, USA (MLP, SM, TFM).

Department of Psychology, University of Nebraska Omaha, 6001 Dodge St., Omaha, NE 68182, USA (ACM, JAF).

MOLECULAR PHARMACOLOGY

SUPPLEMENTARY DATA

Supplementary Table 1.

Line	Ligand	Parameter	Control	Ligand + PTX
mOTR	Leu^8-OT	IC_{50}	63.3 pM	86.5 pM
		95% CI	30.1 to 132.9 pM	26.8 to 279.6 pM
		R^2	0.84	0.67
	Pro^8-OT	IC_{50}	3.2 nM	4.6 nM
		95% CI	0.8 to 13.9 nM	1.0 to 20.7 nM
		R^2	0.59	0.56
hOTR	Leu^8-OT	IC_{50}	109.5 pM	203.9 pM
		95% CI	45.7 to 262.0 pM	74.9 to 552.2 pM
		R^2	0.79	0.76
	Pro^8-OT	IC_{50}	2.2 nM	5.7 nM
		95% CI	1.1 to 4.4 nM	2.1 to 12.3 nM
		R^2	0.85	0.73

Comparison of control and pretreatment with PTX on Leu^8-OT and Pro^8-OT induced membrane hyperpolarization in mOTR and hOTR CHO cells.

Supplementary Table 2.

Line	Parameter	Leu^8-OT	Leu^8-OT+ M119K
mOTR	IC_{50}	5.62 pM	13.9 pM
	95% CI	1.4 to 19.6 pM	1.6 to 119.8 pM
	R^2	0.61	0.45
hOTR	IC_{50}	22.7 pM	121.2 pM
	95% CI	7.1 to 72.5 pM	29.9 to 491.2 pM
	R^2	0.7	0.59

Comparison of control and pretreatment with M1119K on Leu^8-OT induced membrane hyperpolarization in mOTR and hOTR CHO cells.

Supplementary Table 3.

		P-value	
Line	**Inhibitor**	**Leu8-OT**	**Pro8-OT**
mOTR	apamin	<0.0001	0.9994
	charybdotoxin	0.0071	0.9738
	paxilline	0.72	<0.0001
	TRAM-34	<0.0001	<0.0001
	paxilline + TRAM-34	<0.0001	<0.0001
hOTR	apamin	0.0004	0.0016
	charybdotoxin	0.0002	0.0054
	paxilline	<0.0001	<0.0001
	TRAM-34	<0.0001	<0.0001
	paxilline + TRAM-34	<0.0001	<0.0001

Adjusted p-values for Figure 6 (raw data in Supplementary Figures 7-8) one-way ANOVA with Sidek's multiple comparisons test.

Supplementary Table 4.

Line	Paxilline (μM)	P-value	TRAM-34 (nM)	P-value
mOTR	1	0.0090	10	0.2185
	3	<0.0001	30	0.0265
	10	<0.0001	100	<0.0001
	30	<0.0001	300	<0.0001
	100	<0.0001	1000	<0.0001
hOTR	1	0.0043	10	<0.0001
	3	<0.0001	30	<0.0001
	10	<0.0001	100	<0.0001
	30	<0.0001	300	<0.0001
	100	<0.0001	1000	<0.0001

Adjusted p-values for Supplementary Figure 9 one-way ANOVA with Sidek's multiple comparisons test.

Supplementary Table 5.

OTR Region	Position	Amino acid in human	Amino Acid in *Callithrix jacchus*	Substitution type
TM1	47	C; special	S; Neutral/small	Radical
	51	L; Nonpolar/relatively small	F; Nonpolar/relatively large	Conservative
TM4	169	A; Neutral/small	V; Nonpolar/relatively small	Radical
	172	V; Nonpolar/relatively small	M; Nonpolar	Conservative
EC3	193	Q; Neutral	E; Negative	Radical
	197	P; Nonpolar	S; Polar	Radical

Physiochemical change for each amino acid substitution in extracellular and transmembrane domains for *Callithrix jaccus*. TM = Transmembrane, EC = Extracellular

Supplementary Figure 1.

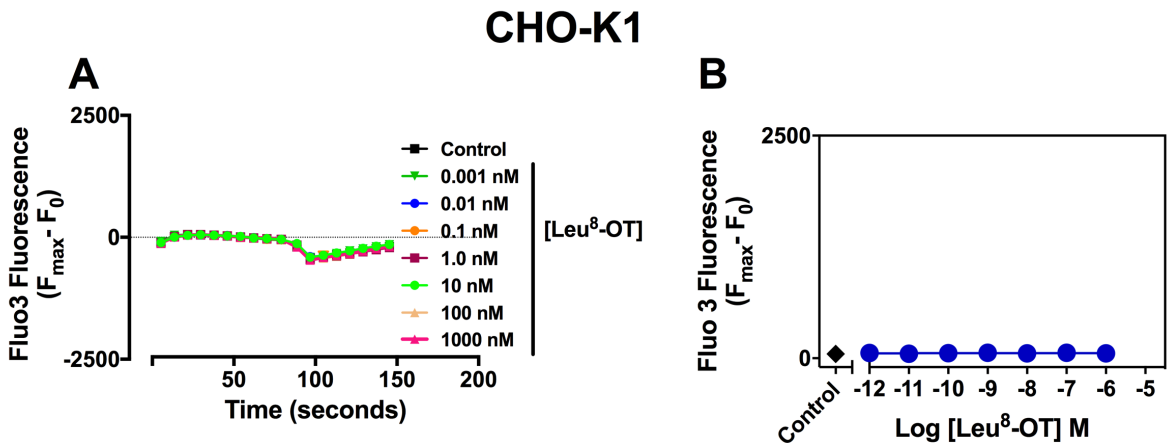

Supplementary Figure 1. Lack of effect of Leu^8-OT on intracellular calcium mobilization in untransfected CHO-K1 cells. Leu^8-OT time-response (A) and concentration-response (B) relationships. N=2 experiments (four replicates per dose per experiment).

Supplementary Figure 2.

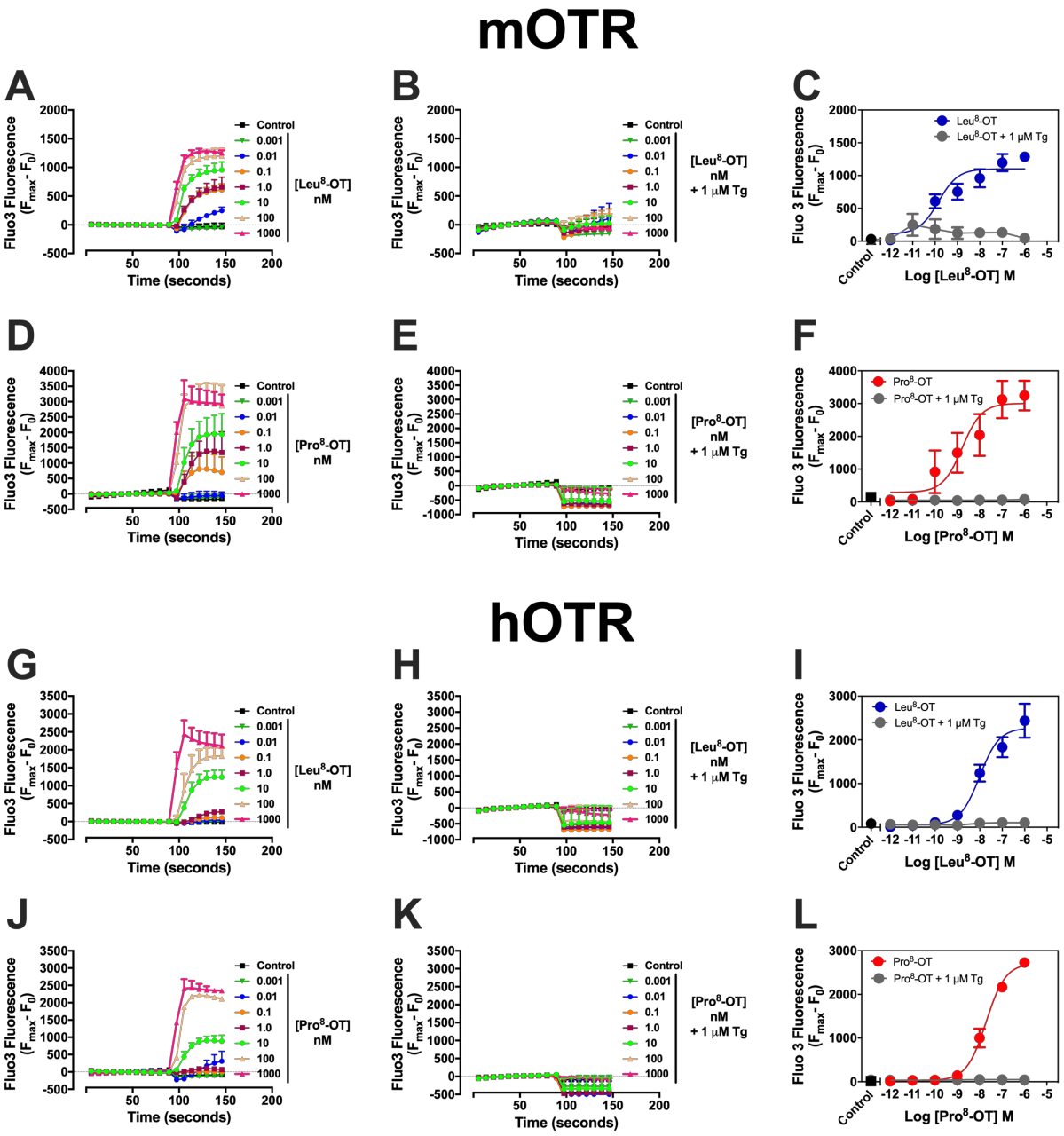

Supplementary Figure 2. Effects of pretreatment with thapsigargin (Tg) on Leu^8-OT and Pro^8-OT induced changes in membrane potential in mOTR and hOTR-expressing CHO cells. Control Leu^8-OT time-response (A) Leu^8-OT time-response in Tg-pretreated cells (B), and concentration-response relationships (C) in mOTR-expressing cells.

Control Pro^8-OT time response (D), Pro^8-OT time response in Tg-pretreated cells (E) and concentration-response relationships (F) in mOTR-expressing cells. Control Leu^8-OT time-response (G) Leu^8-OT time-response in Tg-pretreated cells (H), and concentration-response relationships (I) in hOTR-expressing cells. Control Pro^8-OT time response (J), Pro^8-OT time response in Tg-pretreated cells (K) and concentration-response relationships (L) in hOTR-expressing cells. N=3 experiments and with the same split of cells (five replicates per dose per experiment).

Supplementary Figure 3.

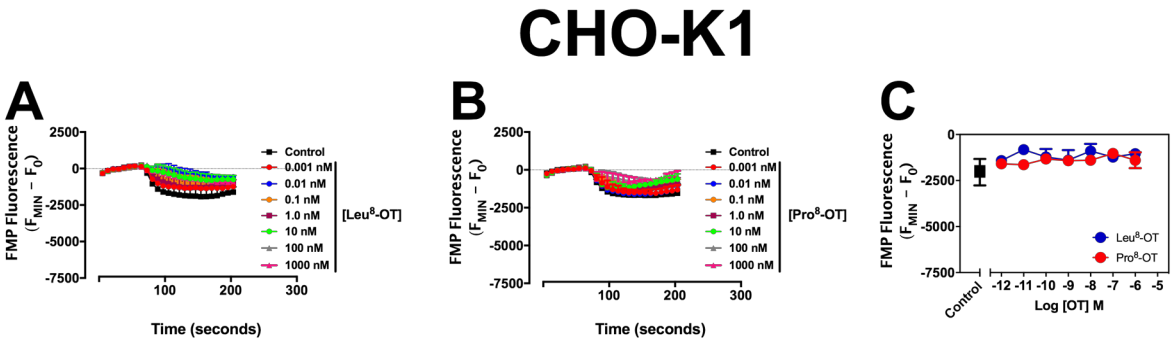

Supplementary Figure 3. Lack of effects of Leu^8-OT and Pro^8-OT on membrane potential in untransfected CHO-K1 cells. Leu^8-OT time-response (A) Pro^8-OT time-response (B) and concentration-response relationships (C). N=2 experiments (five replicates per dose per experiment).

Supplementary Figure 4.

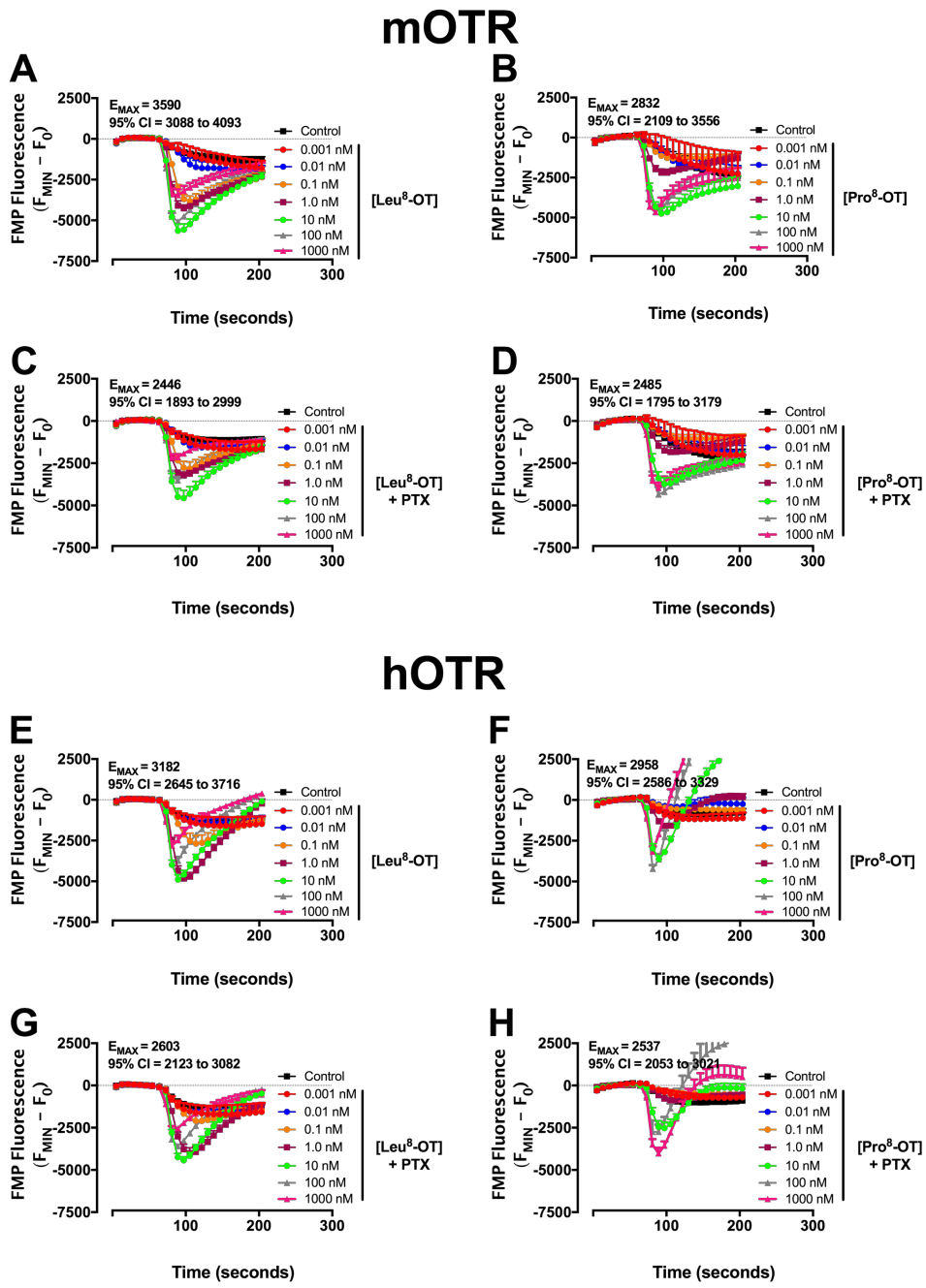

Supplementary Figure 4. Effects of pretreatment with PTX on Leu^8-OT and Pro^8-OT induced changes in membrane potential in mOTR and hOTR-expressing CHO cells. Control Leu^8-OT time-response (A) control Pro^8-OT time-response (B) Leu^8-OT time response in PTX-pretreated (C) Pro^8-OT time-response in PTX-pretreated cells (D) in

mOTR-expressing cells. Control Leu^8-OT time-response (E) control Pro^8-OT time response (F) Leu^8-OT time-response in PTX pretreated (G) Pro^8-OT time-response in PTX-pretreated cells (H) in hOTR-expressing cells. N=6 experiments and with the same split of cells (five replicates per dose per experiment).

Supplementary Figure 5.

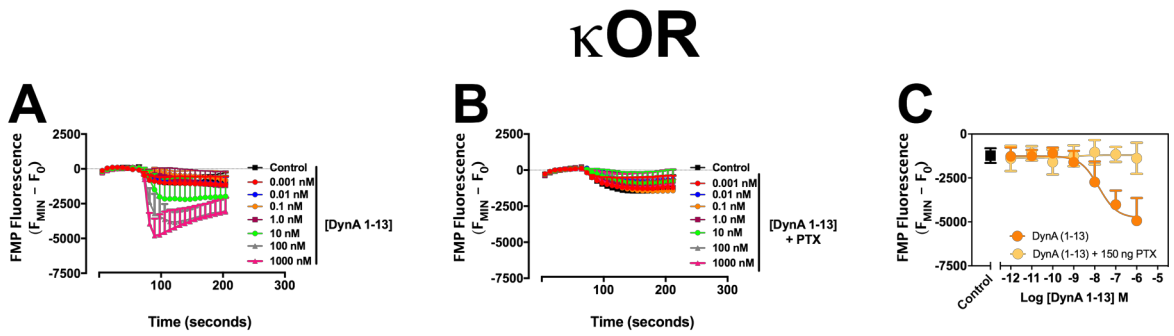

Supplementary Figure 5. Effects of pretreatment with PTX on κOR-CHO cells. Control Dynorphin A (1-13; DynA 1-13) time response (A) DynA 1-13 time-response in PTX-pretreated cells (B) and concentration-response relationships (C). N=3 (five replicates per dose per experiment).

Supplementary Figure 6.

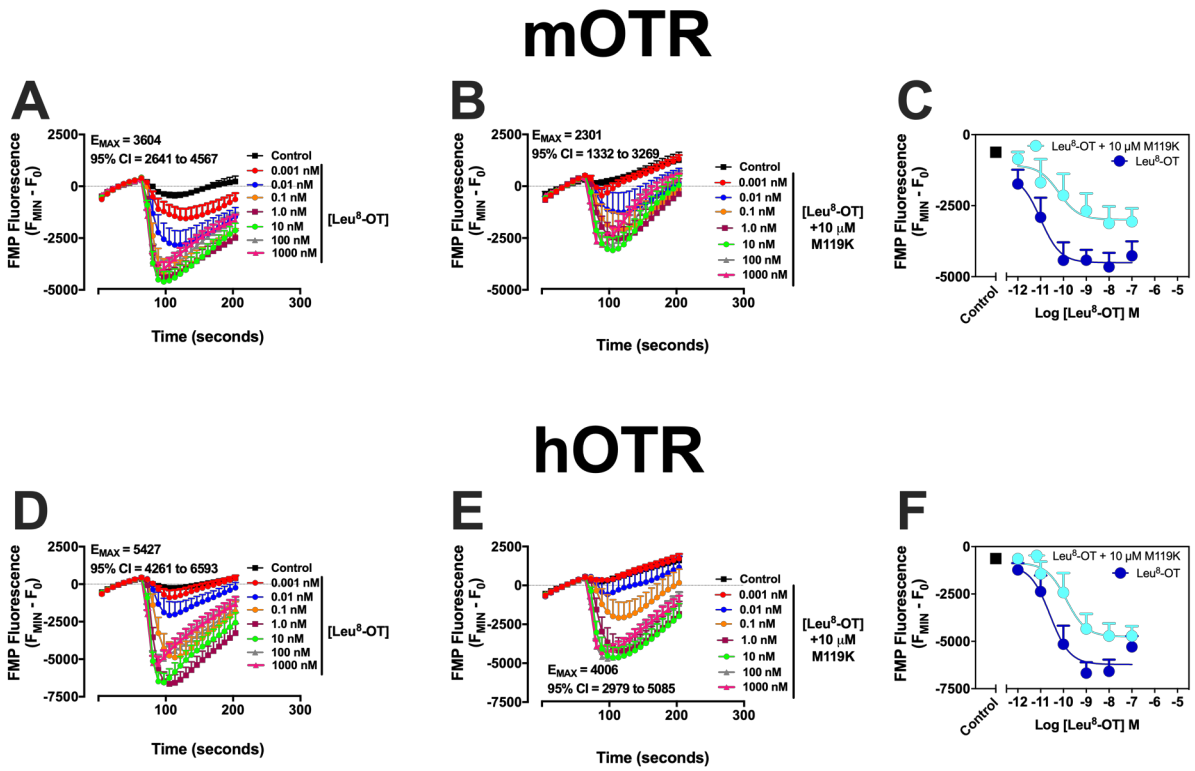

Supplementary Figure 6. Effects of M119K on Leu^8-OT induced changes in membrane potential in mOTR and hOTR-expressing CHO cells. Control Leu^8-OT time-response (A) and Leu^8-OT time-response in M119K-pretreated cells (B) and concentration-response relationships (C) in mOTR-expressing cells. Control Leu^8-OT time-response (E) and Leu^8-OT time-response in M119K-pretreated cells (F) and concentration-response relationships (G) in hOTR-expressing cells. N=6 experiments (five replicates per dose per experiment).

Supplementary Figure 7.

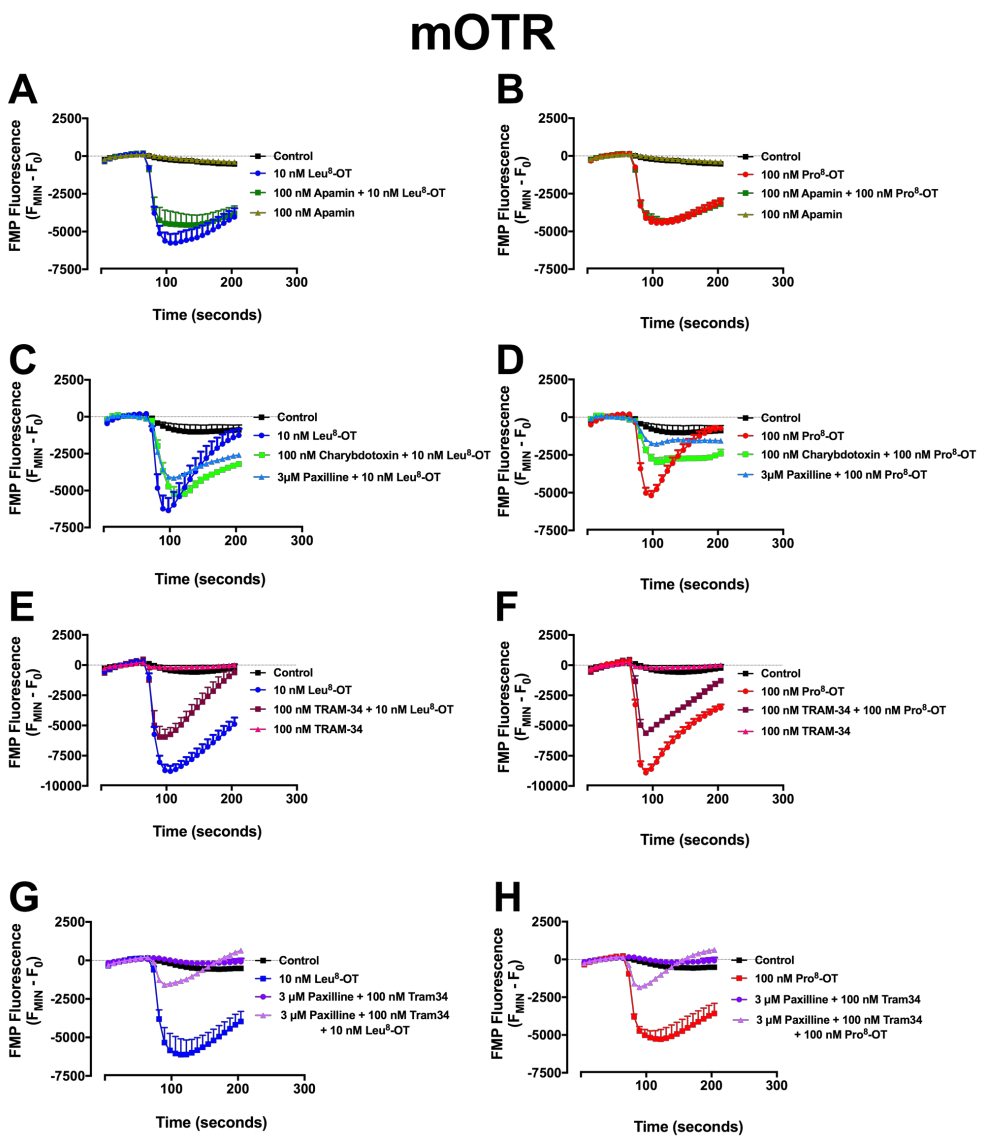

Supplementary Figure 7. Effects of pretreatment with Ca^{2+}-activated K^+ inhibitors on Leu^8-OT or Pro^8-OT induced changes in membrane potential in mOTR-expressing CHO cells. Leu^8-OT +/- SK_{CA} inhibitor apamin (A) and Pro^8-OT +/- SK_{CA} inhibitor apamin (B). Leu^8-OT +/- BK_{CA} inhibitors charybdotoxin or paxilline (C) and Pro^8-OT +/- BK_{CA} inhibitors charybdotoxin or paxilline (D). Leu^8-OT +/- $K_{Ca}3.1$ blocker TRAM-34 (E) and Pro^8-OT +/-). Leu^8-OT +/- $K_{Ca}3.1$ blocker TRAM-34 (F). Leu^8-OT +/- paxilline and TRAM-34 (G) and Pro^8-OT +/- paxilline and TRAM-34 (H). Leu8-OT and Pro8-OT +/- Ca^{2+}-activated K^+ inhibitors were run in parallel on the same plates and with the same split of cells, at the same time for each set of graphs (A-B, C-D, E-F, G-H). N=3 experiments (10 replicates per dose per experiment). Adjusted p-values (Supplementary Table 3).

Supplementary Figure 8.

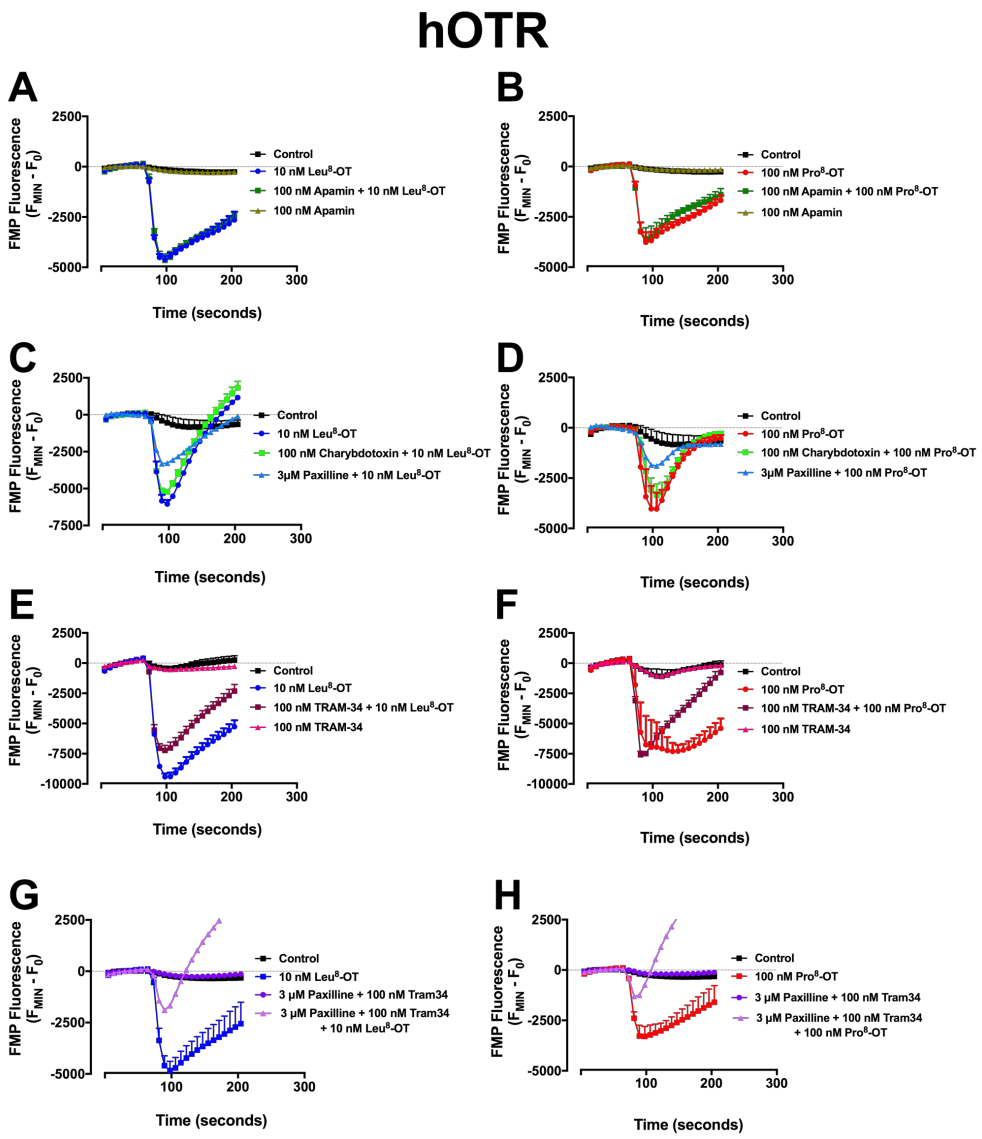

Supplementary Figure 8. Effects of pretreatment with Ca^{2+}-activated K^+ inhibitors on Leu^8-OT or Pro^8-OT induced changes in membrane potential in hOTR-expressing CHO cells. Leu^8-OT +/- SK_{CA} inhibitor apamin (A) and Pro^8-OT +/- SK_{CA} inhibitor apamin (B). Leu^8-OT +/- BK_{CA} inhibitors charybdotoxin or paxilline (C) and Pro^8-OT +/- BK_{CA} inhibitors charybdotoxin or paxilline (D). Leu^8-OT +/- $K_{Ca}3.1$ blocker TRAM-34 (E) and Pro^8-OT +/-). Leu^8-OT +/- $K_{Ca}3.1$ blocker TRAM-34 (F). Leu^8-OT +/- paxilline and TRAM-34 (G) and Pro^8-OT +/- paxilline and TRAM-34 (H). Leu8-OT and Pro8-OT +/-

Ca^{2+}-activated K^+ inhibitors were run in parallel on the same plates, at the same time and with the same split of cells for each set of graphs (A-B, C-D, E-F, G-H). N=3 experiments (10 replicates per dose per experiment). Adjusted p-values (Supplementary Table 3).

Supplementary Figure 9.

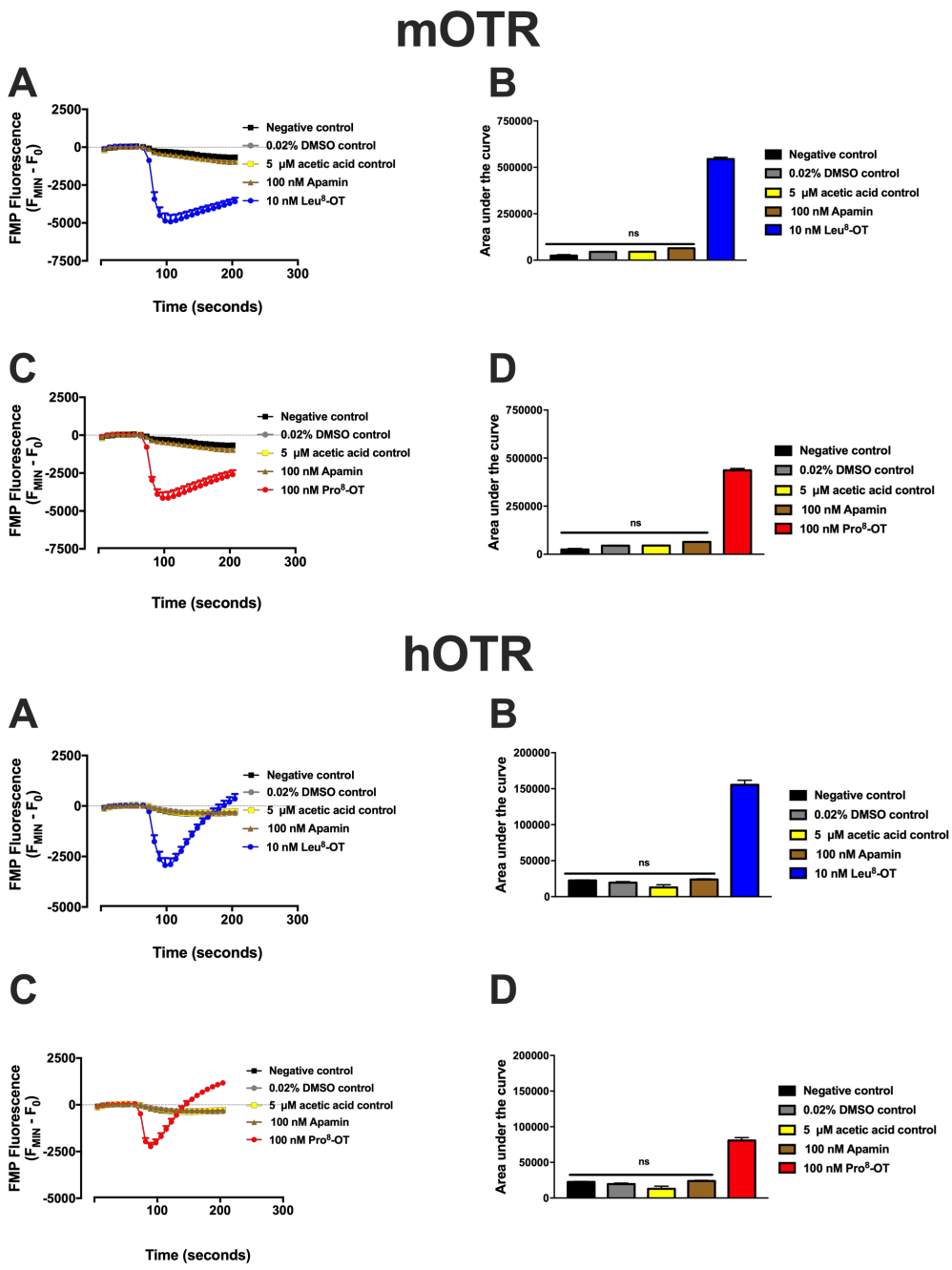

Supplementary Figure 9. Effects of acetic acid solvent on control and OT analog experimental conditions. Controls and Leu^8-OT time response (A) and area under the curve (B) in mOTR cells. Controls and Pro^8-OT time response (C) and area under the curve (D) in mOTR cells. Controls and Leu^8-OT time response (E) and area under the

curve (F) in hOTR cells. Controls and Pro^8-OT time response (G) and area under the curve (H) in hOTR cells. A one-way ANOVA with Sidek's multiple comparisons was performed to determine statistical significance.

Supplementary Figure 10.

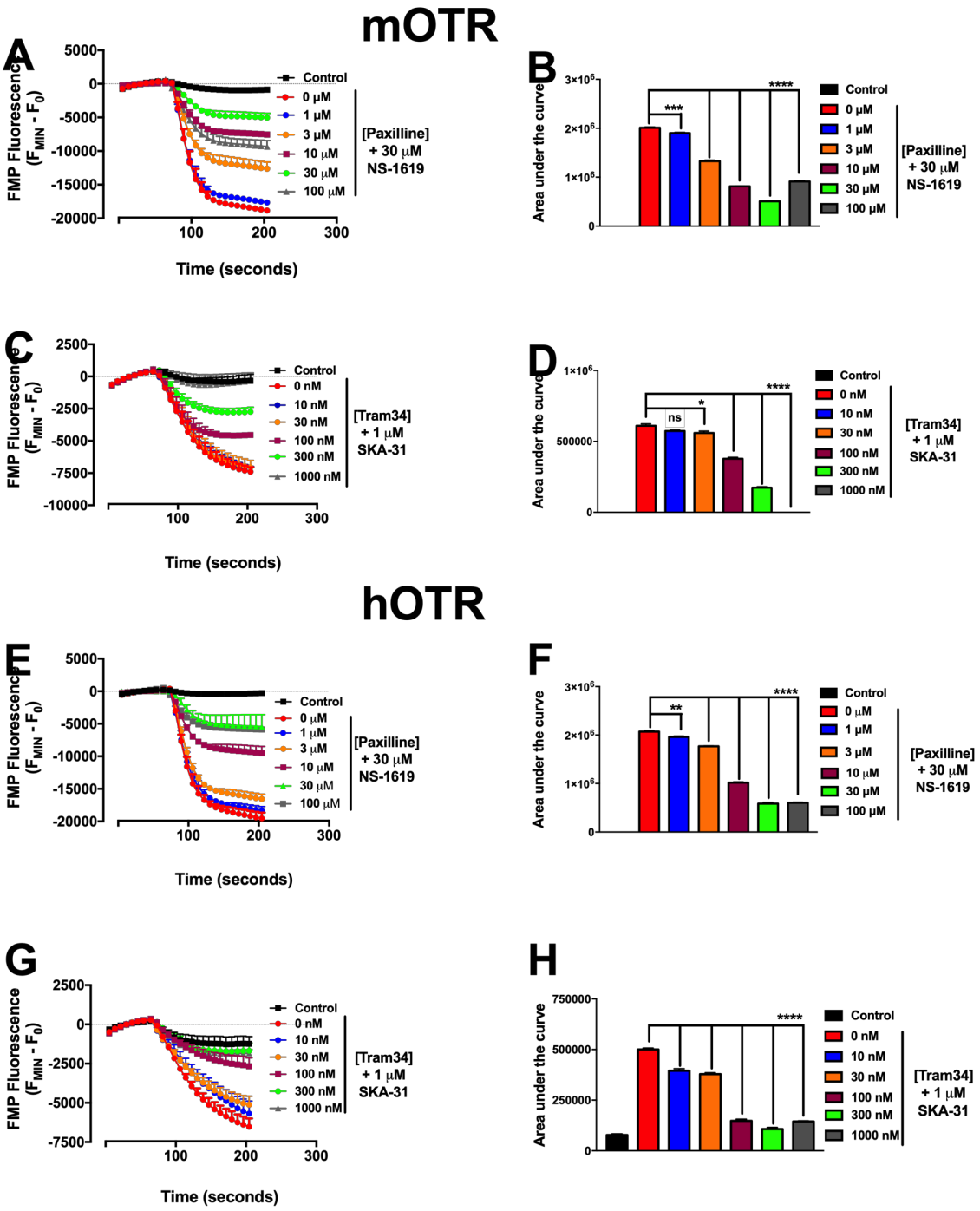

Supplementary Figure 10. Effects of pretreatment with Ca^{2+}-activated potassium channel inhibitors on Ca^{2+}-activated potassium channel activator-induced membrane hyperpolarization in mOTR and hOTR CHO cells. Effects of pretreatment with paxilline

on mOTR NS1619 time response (A) and NS1619 area under the curve (B). Effects of pretreatment with TRAM-34 on mOTR SKA-31 time-response (C) and SKA-31 area under the curve (D). Effects of pretreatment with paxilline on hOTR NS1619 time-response (A) and NS1619 area under the curve (B). Effects of pretreatment with TRAM-34 on hOTR SKA-31 time-response (C) and SKA-31 area under the curve (D). Control and paxilline or TRAM-34-pretreated replicates were run in parallel on the same plates, at the same time. N=3 experiments (10 replicates per dose per experiment). A one-way ANOVA with Sidek's multiple comparisons was used to determine statistical significance. Adjusted p-values (Supplementary Table 4).

Supplementary Figure 11.

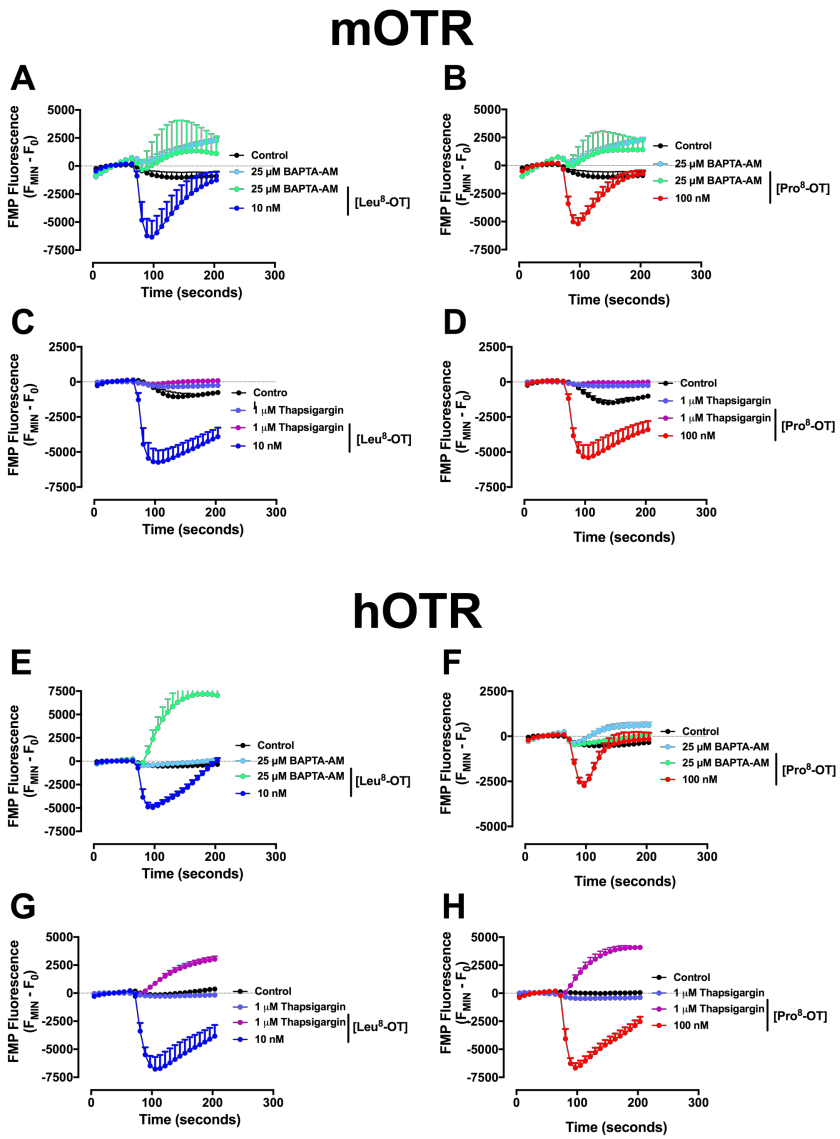

Supplementary Figure 11. Effects of pretreatment with BAPTA-AM and thapsigargin on Leu^8-OT or Pro^8-OT induced changes in membrane potential in mOTR and hOTR-expressing CHO cells. mOTR Leu^8-OT time-response (A, C) and Pro^8-OT time response (B,D). hOTR Leu^8-OT time response (E, G) and Pro^8-OT time-response (F, H). Leu8-OT and Pro8-OT +/- BAPTA-AM or thapsigargin were run in parallel on the same plates, at the same time and with the same split of cells. N=3 experiments (10 replicates per dose per experiment).